# Two-dimensional superconductor in a tilted magnetic field: States with finite Cooper-pair momentum

U. Klein*
*Johannes Kepler Universität Linz, Institut für Theoretische Physik, A-4040 Linz, Austria*
(Received 25 November 2003; published 27 April 2004)

Varying the angle $\theta$ between applied field and the conducting planes of a layered superconductor in a small interval close to the plane-parallel field direction, a large number of superconducting states with unusual properties may be produced. For these states, the pair breaking effect of the magnetic field affects both the orbital and the spin degree of freedom. This leads to pair wave functions with finite momentum, which are labeled by Landau quantum numbers $0<n<\infty$. The stable order-parameter structure and magnetic-field distribution for these states is found by minimizing the quasiclassical free energy near $H_{c2}$ including nonlinear terms. One finds states with coexisting linelike and pointlike order-parameter zeros and states with coexisting vortices and antivortices. The magnetic response may be diamagnetic or paramagnetic depending on the position within the unit cell. The structure of the Fulde-Ferrell-Larkin-Ovchinnikov (FFLO) states at $\theta=0$ is reconsidered. The transition $n\rightarrow\infty$ of the paramagnetic vortex states to the FFLO limit is analyzed and the physical reason for the occupation of higher Landau levels is pointed out.

DOI: 10.1103/PhysRevB.69.134518 PACS number(s): 74.20.Mn, 74.25.Ha, 74.70.Kn

## I. INTRODUCTION

In this paper a theoretical study of a two-dimensional, clean-limit superconductor in a tilted magnetic field is presented. Such systems exist in nature; several classes of layered superconductors of high purity with conducting planes of atomic thickness and nearly perfect decoupling of adjacent planes have been investigated in recent years. These include, among many others, the intercalated transition-metal dichalcogenide $TaS_2$-(pyridine), the organic superconductor $\kappa$-(BEDT-TTF)$_2$Cu(NCS)$_2$, and the magnetic-field-induced superconductor $\lambda$-(BETS)$_2$FeCl$_4$.

Depending on the angle $\theta$ between applied field and conducting planes the nature of the pair-breaking mechanism limiting the superconducting state can be continuously varied. For large $\theta$ the usual orbital pair-breaking mechanism dominates and the equilibrium state is the ordinary vortex lattice. With decreasing $\theta$, in a small interval close to the parallel direction, spin pair breaking becomes of a magnitude comparable to the orbital effect and both mechanisms must be taken into account. For the plane-parallel field direction, $\theta=0$, the orbital effect vanishes completely and the superconducting state is solely limited by paramagnetic pair breaking. The superconducting state expected in this limit is the Fulde-Ferrell-Larkin-Ovchinnikov (FFLO) state.[1,2] The tilted-field arrangement, which allows to control externally the relative strength of both pair-breaking mechanisms, has first been investigated by Bulaevskii.[3]

The upper critical field $H_{c2}$, where a second-order phase transition between the normal-conducting and the superconducting state takes place, has been calculated for arbitrary angle $\theta$ and temperature $T=0$ by Bulaevskii.[3] This treatment was generalized to arbitrary $T$ by Shimahara and Rainer.[4] The field $H_{c2}$ has a cusplike shape, considered both as a function of $\theta$ or $T$, with different pieces of the curve belonging to different values of the Landau quantum number $n$ ($n=0,1,\ldots$). In the orbital pair-breaking regime, for large $\theta$, one finds as expected $n=0$. As is well known, this lowest value $n=0$ determines the (orbital) upper critical field of the familiar vortex state, both in the framework of Ginzburg-Landau (GL) and microscopic theories of superconductivity. With decreasing $\theta$, higher-$n$ segments of the critical-field curve appear close to the plane-parallel orientation. For $\theta\rightarrow 0$ one finds[4] $n\rightarrow\infty$ and agreement with the FFLO upper critical field. Thus, in this purely paramagnetic limit, the stable state below $H_{c2}$ must be the FFLO state.

Paramagnetically limited superconductivity differs in fundamental aspects, such as Meissner effect and spin polarization, from the behavior of the usual, orbitally limited superconducting state. In the FFLO state pairing takes place between electrons with momentum and spin values $(\vec{k}+\vec{q}/2,\uparrow)$ and $(-\vec{k}+\vec{q}/2,\downarrow)$. This leads to Cooper pairs with finite momentum $\hbar\vec{q}$ and a spatially inhomogeneous superconducting order parameter given by $\Delta(\vec{r})=\Delta_0\exp(\imath\vec{q}\vec{r})$ (or by linear combinations of such terms with the same absolute value of $\vec{q}$). The pair breaking is entirely due to the Zeeman coupling between the magnetic moment $\mu$ of the electrons and the external magnetic field $\vec{H}$. The general rule for bulk superconducting states that gradient terms in the free energy must only be taken into account if a nontrivial vector potential is present breaks down for the FFLO state.

At $T=0$, the Cooper-pair momentum of the FFLO state is approximately given by $\hbar q=|p_{F\uparrow}-p_{F\downarrow}|$, where $|p_{F\uparrow}-p_{F\downarrow}|=\mu H\sqrt{2m/E_F}$ is the difference in Fermi momentum between spin-up and spin-down electrons. With increasing $T$ the FFLO wave number $q$ decreases and vanishes at the tricritical point $T_{tri}=0.56\,T_c$. The FFLO state is only stable for $T<T_{tri}$, where its upper critical field $H_{FFLO}$ exceeds the Pauli limiting field $H_P$ of the homogeneous superconducting state.[5,6] At $T=0$, $\mu H_P=\Delta_0/\sqrt{2}$, where $\Delta_0$ is the superconducting gap at $T=0$. The second-order phase transition line $H_{FFLO}(T)$ depends on the shape of the Fermi surface. In this paper we use a cylindrical Fermi surface appropriate for a two-dimensional (2D) geometry. The corresponding critical field[7] is given by $\mu H_{FFLO}=\Delta_0$ at $T=0$.

 

Between the ordinary vortex state with $n=0$ and the FFLO state with $n\to\infty$ a countable infinite number of unconventional superconducting states, characterized by Landau quantum numbers $n=1,2,\ldots$, exist. The transition from the vortex state to the first of these, the $n=1$ state, occurs at an angle $\theta_1$ given approximately by

$$\sin\theta_1 \approx \frac{H_{c2}^{orb}}{H_P} \approx \frac{k_B T_c}{m v_F^2}, \tag{1}$$

where $H_{c2}^{orb}$ and $H_p$ are the ''pure'' orbital and paramagnetic upper critical fields, respectively. Since $H_p \gg H_{c2}^{orb}$, the experimental upper critical field for a three-dimensional sample is given by $H_{c2}^{orb}$. Because $\theta_1 \ll 1$ (generally $\theta_1$ will be of the order of magnitude of 1°), the perpendicular component $H_\perp = H\sin\theta$ for all of these states with $n>0$ will be much smaller than the parallel component $H_\parallel = H\cos\theta$. Thus, these states will have some properties in common with the FFLO state, namely, strong paramagnetic pair breaking, a spatially inhomogeneous order parameter, and Cooper pairs with finite velocity of the center-of-mass coordinate. Despite this similarity with regard to general features, the order-parameter structure for the $n>0$ states may be completely different, even for large $n$, from the FFLO state. The reason is that a finite perpendicular component $H_\perp$, no matter how small, implies a new and rather stringent topological constraint on the equilibrium structure, namely, the flux quantization condition. The subject of the present paper is the detailed investigation of the structure of these $n>0$ states, which might be referred to either as FFLO precursor states or as paramagnetic vortex states, in the vicinity of the upper critical field $H_{c2}$. A theoretical treatment of these FFLO precursor states, reporting several essential results and an outline of the calculation, has been published previously.[8] This paper[8] will be referred to as KRS in what follows. In the present paper many results are reported and the treatment is extended with regard to several points, including finite values of $\kappa$, the purely paramagnetic limit $\theta=0$, and the transition $n\to\infty$.

It should be pointed out that the physical origin of the Landau-level quantization effects for Cooper pairs, considered in the present paper, is very different from the Landau quantization effects for single-electron states discussed in a large number of publications by Tesanovic and co-workers,[9] Rajagopal and co-workers,[10] Norman and co-workers,[11] and others. The latter are mainly concerned with the relative-coordinate degree of freedom of the two bound electrons constituting a Cooper pair and lead to measurable consequences only outside the range of validity of the quasiclassical approximation, at very low temperature $T < (k_B T_c)^2/E_F$ and/or high fields. In addition, a mechanism is required to suppress the Zeeman effect, which is neglected in the theoretical treatment and is not compatible with the predicted phenomena. The question whether the most dramatic consequences[12] (reentrant superconductivity) of this type of Landau quantization effects will be observable, has been the subject of a controversial discussion.[13,14] In contrast, the present Landau-level quantization mechanism is a *consequence* of the Zeeman effect, concerns the center-of-mass motion of the Cooper pairs, and can be described (as will be discussed shortly) by means of the quasiclassical theory of superconductivity.

Restricting ourselves to the vicinity of the upper critical field $H_{c2}$ we may use an expansion of the free energy in powers of the order parameter $\Delta$, keeping only a finite number of terms. An analogous gradient expansion, which would lead to a relatively simple GL-like theory with a finite number of spatial derivatives of $\Delta$, does, unfortunately, not exist for the present problem. Such an expansion may be performed for $\theta=0$, in the purely paramagnetic limit, near the tricritical point $T_{tri}$, where the order-parameter gradient is small because the characteristic length $q^{-1}$ of the FFLO state diverges at $T_{tri}$. However, for finite $H_\perp$ a small characteristic length for order-parameter variations does not exist in the relevant range of temperatures, and the spatial variation of $\Delta$ must be taken into account exactly. One might still hope that a GL theory with a finite number of derivatives, although not accurate, will be useful to predict the *qualitative* behavior of the superconducting states near $H_{c2}$ correctly; bearing in mind, for example, the results of standard GL for type-II superconductivity. However, for the mixed orbital paramagnetic pair-breaking phenomena under discussion, there is not even a single point on the temperature scale where a GL theory with a finite number of derivatives is valid. Such a theory is only valid near $T_c$ where no FFLO state exists, or near $T_{tri}$ in the ''vicinity'' of the paramagnetic limit, i.e., for extremely large $n$. The latter region is inaccessible both from a numerical and a experimental point of view. In this context, it should also be noted that the final equilibrium structures do not show any continuity with regard to $n$.

Fortunately, the present problem does not require solving the full set of Gorkov's equations because the simpler set of quasiclassical equations may be used instead, as pointed out by Bulaevskii.[3] The large parallel component $H_\parallel$ of the applied magnetic field, acting only on the spins of the electrons, is exactly taken into account by the Zeeman term. Thus, with regard to this component no question, as to the validity of the quasiclassical approximation, arises. The magnitude of the perpendicular component $H_\perp$, on the other hand, must obey the usual quasiclassical condition $\hbar\omega_c < k_B T$, where $\omega_c = eH_\perp/mc$, or $\sin\theta(e\hbar H/mc) < k_B T$. Inserting the highest possible field $H=H_P$ in the latter relation, one finds that the quasiclassical approximation holds indeed for not too low temperatures, $T/T_c > k_B T_C/E_F$, in the interesting range of tilt angles $\theta < \theta_1$, where the new paramagnetic vortex states appear.

In most papers on paramagnetic pair breaking and the FFLO state the influence of orbital pair breaking is completely neglected. This means that the GL parameter $\kappa$ tends to infinity and that all spatial variations of the magnetic field can be neglected. For three-dimensional superconductors this approximation implies that the orbital critical field is much higher than the paramagnetic Pauli-limiting field. This is impossible to achieve[15] for BCS-like superconductors, because the superconducting coherence length cannot be smaller than an atomic distance. It seems unlikely even for unconventional materials[16] where many-body effects may lead to a

strong renormalization of the input parameters. For the present two-dimensional (2D) situation, the suppression of the orbital pair-breaking effect is entirely due to geometrical reasons, and no restriction on the value of $\kappa$ is required in order to reach the purely paramagnetic limit at parallel fields. Thus, keeping all terms in the quasiclassical free energy related to spatial variations of the magnetic field will allow us to study type-II superconductors with arbitrary $\kappa$ or even type-I material. Large-$\kappa$ superconductors show, however, still a practical advantage because of their larger critical angle $\theta_1$ [see Eq. (1)].

This paper is organized as follows. In Sec. II Eilenberger's quasiclassical equations generalized with regard to a Zeeman coupling term, as well as the corresponding free-energy functional, are reported. The expansion of the free energy near the upper critical field, for a general 2D quasiperiodic state, is treated in Sec. III. Two limiting cases of the analytical results, the GL limit and the structure of the ordinary vortex lattice, are reported in appendixes. The numerical results for the paramagnetic vortex states, at finite perpendicular field, are reported and discussed in Sec. IV. The structure of the FFLO state, for the special case of vanishing perpendicular field, is reconsidered in the present quasiclassical framework in Sec. V. The nontrivial transition $\theta \to 0$ (or $n \to \infty$) to the purely paramagnetic limit is analyzed in Sec. VI. An explanation for the increase in $n$, in terms of the finite momentum of the Cooper pairs in the paramagnetic vortex states, is also reported in this section. The results are summarized in Sec. VII.

## II. QUASICLASSICAL EQUATIONS WITH ZEEMAN TERM

We need a weak-coupling, clean-limit version of the quasiclassical theory,[17,18] which contains all terms related to the coupling of the electron's spins to an external magnetic field. A general quasiclassical theory which covers Zeeman coupling has been published by Alexander *et al.*[19] The $4\times4$ Green's function matrix appearing in this work may be considerably simplified for the present situation. Since we neglect spin-orbit coupling, the direction of the magnetic induction $\vec{B}$ in spin space may be chosen independently from the direction of $\vec{B}$ in ordinary space; we adopt the usual choice of $\vec{B}$ being parallel to the $z$ direction in spin space. Then, only six essential Green's functions remain, which are denoted by

$$f_{(+)}=f+f_3, \quad f_{(-)}=f-f_3,$$

$$f^+_{(-)}=f^+-f^+_3, \quad f^+_{(+)}=f^++f^+_3,$$

$$g_{(+)}=g+g_3, \quad g_{(-)}=g-g_3.$$

Here, $f$, $f^+$, $g$ denote the Green's functions in the absence of Zeeman coupling, and $f_3$, $f^+_3$, $g_3$ are the additional Green's function components in the $z$ direction of spin space. The three equations for the right group, $f_{(-)}$, $f^+_{(+)}$, $g_{(-)}$, are decoupled from the three equations for the left group, $f_{(+)}$, $f^+_{(-)}$, $g_{(+)}$, and differ only by a negative sign in front of the magnetic moment $\mu \doteq \hbar|e|/(2mc)$ of the electron. Also, for each group separate normalization conditions, $g^2_{(+)}+f_{(+)}f^+_{(-)}=1$ and $g^2_{(-)}+f_{(-)}f^+_{(+)}=1$, respectively, exist. Therefore, it is convenient to introduce Green's functions $f$, $f^+$, $g$, defined by

$$f(\vec{r},\vec{k},\omega_s)=f_{(-)}(\vec{r},\vec{k},\omega),$$

$$f^+(\vec{r},\vec{k},\omega_s)=f^+_{(+)}(\vec{r},\vec{k},\omega),$$

$$g(\vec{r},\vec{k},\omega_s)=g_{(-)}(\vec{r},\vec{k},\omega),$$

which are functions of the spatial variable $\vec{r}$, the quasiparticle wave number $\vec{k}$, and the complex variable $\omega_s=\omega+\imath\mu B$. The 2D variable $\vec{r}$ denotes positions in the conducting $(x,y)$ plane. The real variable $\omega$ takes the values of the Matsubara frequencies $\omega_l=(2l+1)\pi k_B T$; the Matsubara index $l$ will not always be written down explicitly. The second group of Green's functions $f_{(+)}$, $f^+_{(-)}$, $g_{(+)}$ may be expressed by similar relations in terms of $f$, $f^+$, $g$ if $\omega_s$ is replaced by $\omega_s^*$.

Using the Green's functions $f$, $f^+$, $g$, the quasiclassical equations with Zeeman coupling become formally similar to the quasiclassical equations without spin terms. The nonlinear transport equations for $f$, $f^+$ are given by

$$[2\omega_s+\hbar\vec{v}_F(\vec{k})\vec{\partial}_r]f(\vec{r},\vec{k},\omega_s)=2\Delta(\vec{r})g(\vec{r},\vec{k},\omega_s),$$

$$[2\omega_s-\hbar\vec{v}_F(\vec{k})\vec{\partial}^*_r]f^+(\vec{r},\vec{k},\omega_s)=2\Delta^*(\vec{r})g(\vec{r},\vec{k},\omega_s), \quad (2)$$

where the Green's function $g$ is given by the normalization condition

$$g(\vec{r},\vec{k},\omega_s)=[1-f(\vec{r},\vec{k},\omega_s)f^+(\vec{r},\vec{k},\omega_s)]^{1/2}. \quad (3)$$

Here, $\vec{v}_F(\vec{k})$ denotes the Fermi velocity and $\vec{\partial}_r$ is the gauge-invariant derivative defined by $\vec{\partial}_r=\vec{\nabla}_r-\imath(2e/\hbar c)\vec{A}$. The order parameter $\Delta$ and the vector potential $\vec{A}$ must be determined self-consistently.

The self-consistency equation for $\Delta$ is given by

$$\left(2\pi k_B T\sum_{l=0}^{N_D}\frac{1}{\omega_l}+\ln(T/T_c)\right)\Delta(\vec{r})$$

$$=\pi k_B T\sum_{l=0}^{N_D}\oint d^2k'[f(\vec{r},\vec{k}',\omega_s)+f(\vec{r},\vec{k}',\omega_s^*)], \quad (4)$$

where $N_D$ is the cutoff index for the Matsubara sums. The self-consistency equation for $\vec{A}$ is the Maxwell's equation

$$\vec{\nabla}_r\times(\vec{B}(\vec{r})+4\pi\vec{M}(\vec{r}))$$

$$=\frac{16\pi^2 e k_B T N_F}{c}\sum_{l=0}^{N_D}\oint\frac{d^2k'}{4\pi}\vec{v}_F(\vec{k}')\Im g(\vec{r},\vec{k}',\omega_s), \quad (5)$$

where $N_F$ is the normal-state density of states at the Fermi level. The right-hand side (rhs) of Eq. (5) is the familiar

(orbital) London screening current while the magnetization $\vec{M}$ is a consequence of the magnetic moments of the electrons and is given by

$$\vec{M}(\vec{r})=2\mu^2 N_F \vec{B}(\vec{r})-4\pi k_B T N_F \mu \sum_{l=0}^{N_D} \oint \frac{d^2k'}{4\pi} \Im g \frac{\vec{B}}{B}. \tag{6}$$

The first term on the rhs of Eq. (6) is the normal-state spin polarization. The second term is a spin polarization due to quasiparticles in the superconducting state.

The following symmetry relations hold for solutions of Eqs. (2)–(5),

$$\begin{aligned} g^*(\vec{r},-\vec{k},\omega_s^*)&=g(\vec{r},\vec{k},\omega_s),\\ f^+(\vec{r},\vec{k},\omega_s)&=f^*(\vec{r},-\vec{k},\omega_s^*),\\ g(\vec{r},-\vec{k},-\omega_s)&=-g(\vec{r},\vec{k},\omega_s),\\ f(\vec{r},-\vec{k},-\omega_s)&=f(\vec{r},\vec{k},\omega_s),\\ f^+(\vec{r},-\vec{k},-\omega_s)&=f^+(\vec{r},\vec{k},\omega_s), \end{aligned} \tag{7}$$

which have been extensively used in the calculations described in the next sections.

The quasiclassical equations (2), (4), and (5) may be derived as Euler-Lagrange equations of the Gibbs free-energy functional $G$, which is given by

$$G=\frac{1}{F_p}\int d^3r\left[\frac{\vec{B}^2}{8\pi}-\mu^2 N_F \vec{B}^2-\frac{\vec{B}\vec{H}}{4\pi}+N_F\left(\pi k_B T\sum_{l=-\infty}^{+\infty}\frac{1}{|\omega_l|}+\ln(T/T_c)\right)|\Delta|^2-\pi k_B T N_F\sum_{l=-\infty}^{+\infty}\oint\frac{d^2k}{4\pi}I(\vec{r},\vec{k},\omega_s)\right]. \tag{8}$$

The area of the sample is denoted by $F_p$ and the $k$-dependent quantity $I$ is given by

$$I(\vec{r},\vec{k},\omega_s)=\Delta f^+ +\Delta^* f+\left(g-\frac{\omega_l}{|\omega_l|}\right)\left[\frac{1}{f}\left(\omega_s+\frac{\hbar\vec{v}_F}{2}\vec{\partial}_r\right)f+\frac{1}{f^+}\left(\omega_s-\frac{\hbar\vec{v}_F}{2}\vec{\partial}_r^*\right)f^+\right].$$

An important reference state for the present problem is the purely paramagnetically limited homogeneous superconducting state, which is realized for our 2D superconductor if the magnetic field is exactly parallel to the conducting planes. In this case, the vector potential and the gradient terms in the transport equations may be omitted. At $T=0$ the free-energy difference between the superconducting and normal-conducting states may be derived analytically. It is given by

$$G_s-G_n=N_F(\mu^2H^2-\Delta_0^2/2), \tag{9}$$

and vanishes at the Pauli critical field $H_P$. For higher $T$ the self-consistency equation for the gap must be solved numerically, yielding agreement with previous results.[20,7] Let us investigate the magnetic response in this purely paramagnetic limit. It is neglected in most theoretical treatments, but is of particular interest if the influence of finite values of the GL parameter $\kappa$ is to be taken into account. To obtain the magnetization due to the spins, the coupled self-consistency equations (4) and (5) have to be solved. Using dimensionless quantities defined in Appendix A the gap equation takes the form

$$\ln t-t\sum_{l=0}^{N_D}\left[\left(\frac{1}{\sqrt{|\Delta|^2+(\omega_l+\imath\mu B)^2}}+\text{c.c.}\right)-\frac{2}{\omega_l}\right]=0, \tag{10}$$

while Maxwell's equation reduces to

$$B-H=\frac{\mu}{\tilde{\kappa}^2}\left(\mu B-2t\sum_{l=0}^{N_D}\Im\frac{\omega_l+\imath\mu B}{\sqrt{|\Delta|^2+(\omega_l+\imath\mu B)^2}}\right). \tag{11}$$

Note that the orbital screening current [the rhs of Eq. (5)] is completely absent for the plane-parallel field direction. At $T=0$ the rhs of Eq. (11) vanishes exactly. This means that the normal-state spin polarization [first term on the rhs of Eq. (11)] is exactly canceled by the spin polarization due to the superconducting quasiparticles [second term on the rhs of Eq. (11)]. The numerical solution shows that the quasiparticle polarization decreases with increasing $T$ and vanishes at $\Delta=0$, where the magnetic behavior of the normal-conducting state is recovered.

In the rest of this paper dimensionless quantities as introduced by Eilenberger will be used. These quantities are listed in Appendix A. Any exception will be mentioned explicitly.

In the next sections the stable order-parameter structure of a 2D superconductor in the vicinity of the phase boundary will be investigated. The phase boundary $H_{c2}(T)$ itself is given by the highest solution of the equation[4]

$$0=\ln t+t\int_0^\infty ds\frac{1-e^{-\omega_D s}}{\sinh st}\times[1-\cos(\mu Hs)e^{-H_\perp s^2/4}L_n(H_\perp s^2/2)], \tag{12}$$

where the integer $n=0,1,2,\ldots$ is Landau's quantum number, $\omega_D$ is the Debye frequency, and $L_n$ is a Laguerre polynomial[21] of order $n$. A typical phase boundary is shown in Fig. 1. Each piece of the nonmonotonic $H_{c2}$ curve is characterized by a single value of $n$. An infinite number of eigenstates $\phi_{n,k}$ exists, belonging all to the same, highly degenerate eigenvalue $n$. For the present gauge, these are given by

$$\phi_{n,k}(\vec{r})=A\frac{(-1)^n}{\sqrt{n!}}e^{\imath kx}e^{-(H_\perp/2)[y-(k/H_\perp)]^2}\times\text{He}_n\left(\sqrt{2H_\perp}\left[y-\frac{k}{H_\perp}\right]\right), \tag{13}$$

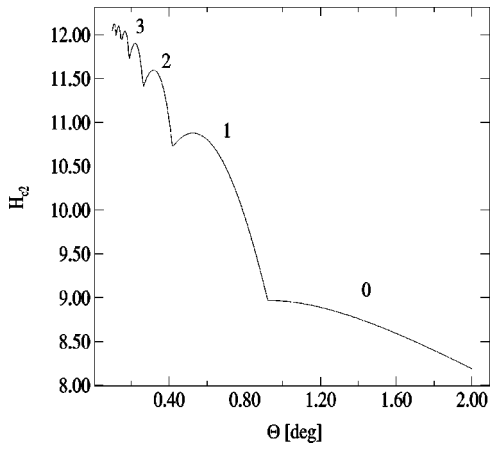


FIG. 1. Phase boundary of the superconducting state at $t=0.1$ for tilt angles $\Theta$ between 0.1 and 2.0 using a value $\mu=0.04$ for the dimensionless magnetic moment of the electron. The numbers 0,1,2,... are Landau quantum numbers characterizing the individual pieces of the curve.

where $k$ is a real number and $\mathrm{He}_n$ is a Hermite polynomial[21] of order $n$. The functions (13) are orthogonal and normalized,

$$(\phi_{n,k},\phi_{m,l})=\delta_{n,m}\delta(k-l), \tag{14}$$

if the amplitude $A$ in Eq. (13) is chosen according to

$$A=\frac{1}{R_0}\left(\frac{H_\perp}{\pi L_x^2}\right)^{1/4}, \tag{15}$$

where $L_x$ is the size of the system in $x$ direction and $R_0$ is defined in Appendix A. The gap, for the portion of the $H_{c2}$ curve characterized by $n$, is a linear combination of all $\phi_{n,k}$ belonging to this $n$. The harmonic-oscillator eigenfunctions (13) are extensively used in the theory of the quantum Hall[22] effect and many other topics in the quantum theory of a charged particle in a magnetic field.

## III. FREE-ENERGY EXPANSION NEAR THE UPPER CRITICAL FIELD

We assume that the transition between the superconducting and normal-conducting states at the upper critical field $H_{c2}$ will be of second order for arbitrary tilt angle $\theta$. Then, the order parameter $\Delta$, or more precisely its amplitude $\epsilon$, may be used as a small parameter for expanding the free energy $G$ in the vicinity of $H_{c2}$. We keep terms up to fourth order in $\epsilon$ and all orders in order-parameter derivatives and determine the energetically most favorable order-parameter structure near $H_{c2}$. Similar calculations for the ordinary vortex lattice, corresponding to the case of large $\Theta$ of the present arrangement, have been performed by Eilenberger[23] and by Rammer and Pesch.[24] No special assumptions on the order-parameter structure, such as the number of zeros per unit cell, will be made. We only assume that the order parameter is quasiperiodic on a 2D lattice, with an arbitrary unit cell, characterized by the length of the two basis vectors and the angle between them. The free energy will be minimized with respect to these unit-cell parameters.

### A. Order parameter

Let the unit vector $\vec{a}$ of our elementary cell be parallel to the $x$ axis, $\vec{a}=a\vec{e}_x$. The angle between $\vec{a}$ and the second unit vector $\vec{b}$ is denoted by $\alpha$. To construct a quasiperiodic order parameter near $H_{c2}$, exactly the same method as used by Abrikosov,[25] for the case $n=0$, may be applied. The result is given by the following linear combination of a subset of the basis functions (13):

$$\Delta_n(\vec{r})=AC_n\sum_{m=-\infty}^{m=+\infty}\exp\left(-\imath\pi\frac{b}{a}m(m+1)\cos\alpha\right)\times\exp\left(\imath\frac{2\pi}{a}mx\right)h_n(y-mb\sin\alpha), \tag{16}$$

where

$$h_n(z)=\frac{(-1)^n}{\sqrt{n!}}e^{-(\bar{B}_\perp/2)z^2}\mathrm{He}_n(\sqrt{2\bar{B}_\perp}z).$$

This order parameter[8,11,26] is not invariant under translations $\vec{r}\to\vec{r}'=\vec{r}+n\vec{a}+m\vec{b}$ but acquires phase factors for each elementary translation, which are uniquely defined within a fixed gauge. Surrounding a unit cell in counterclockwise direction, these phase changes add up to a total factor of $\exp\imath 2\pi$, i.e., each unit cell carries a single flux quantum $\Phi_0$. We shall use this assumption of a single flux quantum per unit cell, which is written as $\bar{B}_\perp ab\sin\alpha=2\pi$ in the present units, throughout this paper. Preliminary calculations[27] show that states with two flux quanta per unit cell have higher free energy and can be excluded. Also, a preference for multiquanta vortices seems unlikely in the present situation, where the single flux quantum state is stable at large $\Theta$, while the total flux decreases to zero as $\Theta\to 0$.

The order parameter (16) describes a flux-line lattice where the Cooper-pair states belong to arbitrary Landau quantum numbers $n$, depending on the tilt angle $\Theta$. As is well known, the pairing states for the ordinary vortex state belong to the lowest Landau level $n=0$. The present shift to higher Landau levels is, of course, related to the large paramagnetic pair-breaking field $H_\parallel$ as will be discussed in more detail in Sec. VI.

The coefficient $C_n$ in Eq. (16) may be expressed by the spatial average of the square of the order parameter, using the relation

$$\langle|\Delta_n|^2\rangle=\frac{1}{F_p}|C_n|^2\sum_{m=-M/2}^{+M/2}1, \tag{17}$$

where $F_p$ is the area of the sample. The spatial average over the unit-cell area $F_c=ab\sin\alpha$ is defined in Appendix A. For later use, when performing the limit $\Theta\to 0$ in Sec. VI, we assumed in Eq. (17) that the area of the superconducting plane is finite and that the number of unit cells in one direction is $M$. At the end of the following calculation, $C_n$ will be

fixed according to the requirement $\langle|\Delta_n|^2\rangle=1$ and an infinitesimal amplitude $\epsilon$ will be attached in front of each power of $\Delta_n$.

A useful quantity is the square of the order-parameter modulus, which may be written in the form

$$|\psi_n|^2(\vec{r})=\sum_{l,j}\ (\psi_n^2)_{l,j}e^{\imath\vec{Q}_{l,j}\vec{r}}. \tag{18}$$

The Fourier coefficients $(\psi_n^2)_{l,j}$ are given by

$$(\psi_n^2)_{l,j}=(-1)^{lj}e^{-\imath\pi l(b/a)\cos\alpha}e^{-x_{l,j}/2}L_n(x_{l,j}), \tag{19}$$

where $x_{l,j}$ is defined by Eq. (B4). The order parameter $\psi_n$ is proportional to $\Delta_n$ but with an amplitude chosen according to $\langle|\psi_n|^2\rangle=1$. It is instructive to compare Eq. (18) with the local magnetic field reported later in Sec. III E.

### B. General aspects of the expansion

A fourth-order expansion of $G$ requires first- and third-order contributions in the Green's functions $f$, $f^+$. We use the notation

$$f=f^{(1)}+f^{(3)},\quad f^+=f^{+(1)}+f^{+(3)}, \tag{20}$$

where $f^{(1)}$ and $f^{(3)}$ are the contributions of order $\epsilon^1$ and $\epsilon^3$, respectively. A consistent treatment of the magnetic-field terms[28,29] requires a separation of $\vec{B}$ and $\vec{A}$ according to

$$\vec{B}(\vec{r})=\overline{\vec{B}}+\vec{B}_1(\vec{r}),\quad \vec{A}(\vec{r})=\overline{\vec{A}}(\vec{r})+\vec{A}_1(\vec{r}), \tag{21}$$

where $\overline{\vec{B}}$ is the spatially constant magnetic induction, $\vec{B}_1(\vec{r})$ is the $\vec{r}$-dependent deviation from $\overline{\vec{B}}$ and $\overline{\vec{A}}(\vec{r})$, and $\vec{A}_1(\vec{r})$ are the corresponding vector potentials. An evaluation of the magnetic-field terms in $G$ requires the leading order in $\vec{B}_1(\vec{r})$, which is $\epsilon^2$: $\vec{B}_1\approx\vec{B}_1^{(2)}$. The spatially constant quantity $H_{c2}-\overline{B}$, where $\overline{B}=|\overline{\vec{B}}|$, is small of order $\epsilon^2$. The whole expansion in $\epsilon$ will be done keeping $\overline{B}$ fixed; at the end of the calculation, the Gibbs free energy $G$ will be minimized with respect to the order-parameter amplitude $\epsilon$ and the induction $\overline{B}$. The calculation can be seen as an extension of Abrikosov's classical work[25] to arbitrary temperatures below $T_c$.

Let us choose the coordinate system in such a way that the magnetic field lies in the $(y,z)$ plane. Then, the induction $\vec{B}(\vec{r})$ (and the external field $\vec{H}$) may be split according to

$$\vec{B}(\vec{r})=B_\parallel(\vec{r})\vec{e}_y+B_\perp(\vec{r})\vec{e}_z, \tag{22}$$

in perpendicular and parallel components $B_\perp$, $B_\parallel$. The corresponding vector potentials are denoted by $\vec{A}_\perp$, $\vec{A}_\parallel$. In order to fix the gauge we may employ here essentially the same method as used before in numerical calculations on the vortex lattice without Zeeman coupling.[29,30] The gauge conditions which fix $\vec{A}_1$ are given by[28]

$$\frac{\partial\vec{A}_1}{\partial\vec{r}}=0,\quad \int d^2r\vec{A}_1=0,\quad \vec{A}_1\ \text{periodic}. \tag{23}$$

The vector potential $\overline{\vec{A}}$ describing the average value $\overline{\vec{B}}$ of the induction is chosen according to

$$\overline{\vec{A}}(\vec{r})=(\overline{B}_\parallel z-\overline{B}_\perp y)\vec{e}_x. \tag{24}$$

The first term in Eq. (24) can be omitted in the gauge-invariant derivatives of Eq. (2) since no $z$ dependence exists in our 2D system. Thus, the orbital pair-breaking contribution in the transport equations consists of the sum of the second term $\propto\overline{B}_\perp$ in Eq. (24) and the $\vec{r}$-dependent part $\vec{A}_1$ (only the perpendicular component of $\vec{A}_1$ is relevant here). The (large) parallel component $\overline{B}_\parallel$, on the other hand, enters the spin pair-breaking term, which is proportional to $B(\vec{r})=[B_\parallel^2(\vec{r})+B_\perp^2(\vec{r})]^{1/2}$. Equations (23) and (24) fix the gauge, i.e., allow a unique determination of $\vec{A}$ in terms of $\vec{B}$. While $|\Delta|^2$ and $\vec{B}$ are periodic, i.e., invariant under translations between equivalent points in the 2D structure, $\Delta$ and $\vec{A}$ are only quasiperiodic, i.e., they differ by phase factors and a change in gauge, respectively. The phase factors are fixed within a given gauge and may be calculated using Eq. (24).

As a first step in the expansion of $G$, the Green's function $g$ is eliminated in favor of $f$, $f^+$ by means of the relation

$$g=1-\frac{ff^+}{2}-\frac{f^2(f^+)^2}{8}+\ \ldots,$$

which is valid for small $\Delta$. Second, the gradient terms in $G$ may be eliminated with the help of the transport equations (2). Then, the (dimensionless) Gibbs free energy takes the form

$$G=\frac{1}{F_p}\int d^3r\Bigg(\tilde{\kappa}^2(\vec{B}-\vec{H})^2-\mu^2\vec{B}^2+\left(\ln t+2\sum_{l=0}^{\infty}\frac{1}{2l+1}\right)\times|\Delta|^2-\frac{t}{2}\sum_{l=0}^{\infty}\Bigg[\Delta\overline{f^+}+\Delta^*\overline{f}+\frac{1}{4}[\Delta\overline{f(f^+)^2}+\Delta^*\overline{f^2f^+}]+\text{c.c.}\Bigg]\Bigg), \tag{25}$$

where the bar denotes a Fermi-surface average as defined in Appendix A. In divergent Matsubara sums, like the one in Eq. (25), the upper, infinite limit of $l$ has been replaced by a finite cutoff using the standard method.

Inserting the expansions (20) and (21) in the free energy (25) and collecting terms of the same order in $\epsilon$, $G$ takes the form

$$G=\overline{G}+G^{(2)}+G^{(4)}, \tag{26}$$

where the terms $\overline{G}$, $G^{(2)}$, and $G^{(4)}$ denote the free energy contributions of order $\epsilon^0$, $\epsilon^2$, and $\epsilon^4$, respectively. The term $\overline{G}$ is given by

$$\overline{G}=\tilde{\kappa}^2(\overline{\vec{B}}-\vec{H})^2-\mu^2\overline{\vec{B}}^2. \tag{27}$$

We will first simplify the quantities $G^{(2)}$ and $G^{(4)}$ and then calculate the minimum of $G$ with respect to the amplitude $\epsilon$ and the induction $\overline{B}$.

### C. Second-order contribution

The second-order contribution to the Gibbs free energy is given by

$$G^{(2)}=\frac{1}{A}\int d^3r\left[\left(\ln t+2\sum_{l=0}^{\infty}\frac{1}{2l+1}\right)|\Delta|^2-\frac{t}{2}\sum_{l=0}^{\infty}(\Delta\overline{f^{+(1)}}+\Delta^*\overline{f^{(1)}}+\text{c.c.})\right]. \tag{28}$$

To calculate the lowest-order Green's function only contributions of order $\epsilon^0$, namely the spatially constant part $\overline{B}=(\overline{B_\parallel^2}+\overline{B_\perp^2})^{1/2}$ of the induction and the lowest-order vector potential $\vec{\overline{A}}$, have to be taken into account in Eq. (2). The resulting equation for $f^{(1)}$ is given by

$$[\omega_l+\imath\mu\overline{B}+\hat{k}\vec{\partial}_r^{(0)}]f^{(1)}=\Delta, \tag{29}$$

where $\vec{\partial}_r^{(0)}=(\partial/\partial\vec{r})+\imath\overline{B}_\perp y\vec{e}_x$. To proceed, we use well-known methods[31] and solve first the eigenvalue problem of the operator $\hat{k}\vec{\partial}_r^{(0)}$. The solution is given by

$$\hat{k}\vec{\partial}_r^{(0)}f_{\hat{k},\vec{p}}(\vec{r})=E_{\hat{k},\vec{r}}f_{\hat{k},\vec{p}}(\vec{r}), \tag{30}$$

with the eigenvalues $E_{\hat{k},\vec{r}}=\imath\hat{k}\vec{p}$ and the eigenfunctions

$$f_{\hat{k},\vec{p}}(\vec{r})=\exp\left[\imath\frac{\overline{B}_\perp}{2}(x\hat{k}_x+y\hat{k}_y)(x\hat{k}_y-y\hat{k}_x)-\imath\overline{B}_\perp\frac{xy}{2}+\imath\vec{p}\vec{r}\right]. \tag{31}$$

Using the completeness of this continuous set of eigenfunctions the differential operator on the left-hand side (lhs) of Eq. (29) may be inverted and $f^{(1)}$ be represented in the form

$$f^{(1)}=\int\frac{d^2p}{4\pi^2}\int d^2r_1\frac{f_{\hat{k},\vec{p}}(\vec{r})f^*_{\hat{k},\vec{p}}(\vec{r}_1)}{\omega_l+\imath\mu\overline{B}+\imath\hat{k}\vec{p}}\Delta(\vec{r}_1). \tag{32}$$

Representing the denominator in Eq. (32) by means of the identity

$$\frac{1}{r}=\int_0^\infty dse^{-sr} \tag{33}$$

as an additional integral, both the $\vec{p}$ integration and the $\vec{r}_1$ integration may be performed analytically and the solution of Eq. (29) takes the form

$$f^{(1)}(\hat{k},\omega_s,\vec{r})=\int_0^\infty due^{-u\omega_s}\exp\left[\imath\frac{\overline{B}}{2}(-2uy\hat{k}_x+u^2\hat{k}_x\hat{k}_y)\right]\Delta^*(\vec{r}-u\hat{k}). \tag{34}$$

The first-order solution for $f^+$ is given by $f^{+(1)}(\hat{k},\omega_s,\vec{r})=f^{(1)*}(-\hat{k},\omega_s^*,\vec{r})$.

The evaluation of the remaining integrals may be greatly simplified by introducing the gap correlation function $V(\vec{r}_1,\vec{r}_2)$. In the present gauge it is defined by

$$V(\vec{r}_1,\vec{r}_2)=\Delta(\vec{r}_1)\Delta^*(\vec{r}_2)\exp\left[\imath\frac{\overline{B}_\perp}{2}(x_1-x_2)(y_1+y_2)\right]. \tag{35}$$

Of particular importance are the Fourier coefficients $V_{l,j}(\vec{r})$, where $\vec{r}=\vec{r}_1-\vec{r}_2$. The precise definition and calculation of $V_{l,j}(\vec{r})$ is reported in Appendix B.

All terms in Eq. (28) containing first-order Green's functions may be expressed as integrals over a gap correlation function. The first of these takes the form

$$\Delta f^{+(1)}=\int_0^\infty due^{-u\omega_s}V^*(\vec{r}+u\hat{k},\vec{r}), \tag{36}$$

while the corresponding expression for $\Delta^*f^{(1)}$ may be derived from Eq. (36) with the help of the symmetry relations (7). To proceed, center-of-mass coordinates are introduced and a Fourier expansion of $V^{CM}(\vec{R},\vec{r})$ with regard to the variable $\vec{R}$ is performed, using the result (B3) from Appendix B. The remaining summations and integrations may be performed analytically.[21] Collecting all terms one obtains the final result for the second-order contribution

$$G^{(2)}=\langle|\Delta|^2\rangle\left[\ln t+t\int_0^\infty ds\frac{1-e^{-\omega_D s}}{\sinh st}[1-\cos(\mu\overline{B}s)\times e^{-\overline{B}_\perp s^2/4}L_n(\overline{B}_\perp s^2/2)]\right]. \tag{37}$$

While the order parameter expansion, Eq. (16), which entered the calculation of $G^{(2)}$, depends on the lattice parameters $a,b,\alpha$, this dependence is absent in the final result, Eq. (37). The quantity $G^{(2)}$, characterizing the appearance of the superconducting instability, and not the detailed structure below it, does only depend on the eigenvalue $n$. The relation $G^{(2)}=0$ agrees with the linearized gap equation (12) used to calculate $H_{c2}$.

The technique used here to calculate $G^{(2)}$ will be generalized in the following section to evaluate the fourth-order contribution to the free energy.

### D. Fourth-order contribution

The free-energy contribution of order $\epsilon^4$ may be split, according to

$$G^{(4)}=G_N^{(4)}+G_M^{(4)}, \tag{38}$$

in a nonmagnetic part $G_N^{(4)}$ and a magnetic part $G_M^{(4)}$. In $G_N^{(4)}$ the spatially constant induction $\overline{B}$ and the corresponding vector potential $\vec{\overline{A}}(\vec{r})$ are used. The term $G_M^{(4)}$ collects all terms of order $\epsilon^4$ where deviations $\vec{B}_1(\vec{r})\approx\epsilon^2$ [or the correspond-

ing vector potential $\vec{A}_1(\vec{r})]$ from the average induction $\overline{\vec{B}}$ are taken into account; for $\kappa\to\infty$, it becomes negligibly small.

The nonmagnetic part $G_N^{(4)}$ is given by

$$G_N^{(4)}=G_a^{(4)}+G_b^{(4)}. \tag{39}$$

The term $G_a^{(4)}$ may be calculated using the solutions $f^{(1)}$, $f^{+(1)}$ of order $\epsilon^1$, already obtained in Sec. III C,

$$G_a^{(4)}=-\left\langle \frac{t}{8}\sum_{l=0}^{N_D}[\Delta^*\overline{f^{(1)2}f^{+(1)}}+\Delta\overline{f^{(1)}f^{+(1)2}}+\text{c.c.}]\right\rangle. \tag{40}$$

The term $G_b^{(4)}$ requires the nonmagnetic parts $f_N^{(3)}$, $f_N^{+(3)}$ of the third-order Green's functions $f^{(3)}$, $f^{+(3)}$,

$$G_b^{(4)}=-\left\langle \frac{t}{2}\sum_{l=0}^{N_D}[\Delta^*\overline{f_N^{(3)}}+\Delta\overline{f_N^{+(3)}}+\text{c.c.}]\right\rangle. \tag{41}$$

The magnetic part $G_M^{(4)}$ is given by

$$G_M^{(4)}=G_c^{(4)}+G_d^{(4)}. \tag{42}$$

The term $G_c^{(4)}$ is purely magnetic in origin, while the term $G_d^{(4)}$ contains the magnetic parts $f_M^{(3)}$, $f_M^{+(3)}$ of the third-order Green's functions,

$$G_c^{(4)}=\langle(\tilde{\kappa}^2-\mu^2)\vec{B}_1^2\rangle, \tag{43}$$

$$G_d^{(4)}=-\left\langle \frac{t}{2}\sum_{l=0}^{N_D}[\Delta^*\overline{f_M^{(3)}}+\Delta\overline{f_M^{+(3)}}+\text{c.c.}]\right\rangle. \tag{44}$$

In a next step, the terms $\vec{B}_1$ and $f^{(3)}=f_N^{(3)}+f_M^{(3)}$ of order $\epsilon^2$ and $\epsilon^3$, respectively, must be calculated. The same method used in Sec. III C to calculate $f^{(1)}$, by inverting the differential operator on the lhs of Eq. (29), may be used here to obtain $f^{(3)}$. Using an operator notation for brevity, the sum of $f_N^{(3)}$ and $f_M^{(3)}$ may be written as

$$f^{(3)}=[\omega_l+\imath\mu\overline{B}+\hat{k}\vec{\partial}_r^{(0)}]^{-1}D, \tag{45}$$

$$D=-\frac{1}{2}\Delta f^{(1)}f^{+(1)}-Pf^{(1)}. \tag{46}$$

The first and second term in Eq. (46) gives $f_N^{(3)}$ and $f_M^{(3)}$, respectively. The term $P$ is of order $\epsilon^2$ and is given by

$$P=\imath\frac{\mu}{\overline{B}}\overline{\vec{B}\vec{B}_1^{(2)}}-\imath\hat{k}\vec{A}_1^{(2)}. \tag{47}$$

The magnetic contributions $\vec{B}_1=\vec{B}_1^{(2)}$ and $\vec{A}_1^{(2)}$ must be determined by solving Maxwell's equation (5). Expanding Eq. (5) one obtains two decoupled equations,

$$\left(1-\frac{\mu^2}{\tilde{\kappa}^2}\right)\vec{B}_{1\parallel}=-\eta^0\overline{\vec{B}}_{\parallel}, \tag{48}$$

$$\vec{\nabla}_r\times\left[\left(1-\frac{\mu^2}{\tilde{\kappa}^2}\right)\vec{B}_{1\perp}+\eta^0\overline{\vec{B}}_{\perp}\right]=\vec{\beta}, \tag{49}$$

for the parallel and perpendicular components $\vec{B}_{1\parallel}$ and $\vec{B}_{1\perp}$ of $\vec{B}_1$. The quantities $\eta^0$, $\vec{\beta}$, which are both of order $\epsilon^2$, are given by

$$\eta^0=\frac{t}{\overline{B}}\frac{2\mu}{\tilde{\kappa}^2}\sum_{l=0}^{N_D}\overline{\mathfrak{I}g},\quad \vec{\beta}=\frac{2t}{\tilde{\kappa}^2}\sum_{l=0}^{N_D}\overline{\hat{k}\mathfrak{I}g}. \tag{50}$$

The Green's function $g$ in Eq. (50) may be replaced by $-f^{(1)}f^{+(1)}/2$ under the $\hat{k}$ integral. Thus, $\eta^0$, $\vec{\beta}$ may be calculated by using the first-order solutions $f^{(1)}$, $f^{+(1)}$ as given by Eq. (34). The solution of Eqs. (48) and (49) is obtained by expanding the unknown variables $\vec{B}_{1\parallel}$, $\vec{B}_{1\perp}$ and the parameters $\eta^0$, $\vec{\beta}$, which are all invariant under lattice translations, in Fourier series; the corresponding Fourier coefficients are denoted by $(\vec{B}_{1\parallel})_{l,m}=(B_{1\parallel})_{l,m}\vec{e}_y$, $(\vec{B}_{1\perp})_{l,m}=(B_{1\perp})_{l,m}\vec{e}_z$, and $(\eta^0)_{l,m}$, $\vec{\beta}_{l,m}$. The explicit solutions will be reported at the end of this section.

Given the second-order contribution $\vec{B}_1$, the first term $G_c^{(4)}$ of $f_M^{(3)}$ [see Eq. (43)] can be evaluated. To calculate the second term $G_d^{(4)}$ one needs, in addition, the correction term $\vec{A}_1$ [see Eqs. (45)–(47)]. Writing $\vec{A}_1=\vec{A}_{1\parallel}+\vec{A}_{1\perp}$, the Fourier coefficients of $\vec{A}_{1\parallel}$, $\vec{A}_{1\perp}$ may be expressed[29] in terms of the Fourier coefficients of the induction,

$$(\vec{A}_{1\parallel})_{l,m}=\frac{\imath}{\tilde{Q}_{l,m}^2}Q_{l,m,x}(B_{1\parallel})_{l,m}\vec{e}_z,$$

$$(\vec{A}_{1\perp})_{l,m}=\frac{\imath}{\tilde{Q}_{l,m}^2}(B_{1\perp})_{l,m}(Q_{l,m,y}\vec{e}_x-Q_{l,m,x}\vec{e}_y), \tag{51}$$

using the gauge conditions defined by Eq. (23). The quantities $Q_{l,m,x}$, $Q_{l,m,y}$ in Eq. (51) are the $x$ and $y$ components of the reciprocal lattice vector $\vec{Q}_{l,m}$ defined in Appendix B.

Each one of the four terms of order $\epsilon^4$ in Eqs. (39) and (42) may be represented as a multiple integral and Matsubara sum over the product of *two* gap correlation functions. What remains to be done is to perform analytically as many integrations as possible. The details of the calculation will be reported here for the first term $G_a^{(4)}$, defined by Eq. (40); the evaluation of the other three terms is similar.

Using the first-order Green's functions (34) and the definition of the gap correlation function (35), the term $G_a^{(4)}$ takes the form

$$G_a^{(4)}=-\left\langle \frac{t}{8}\sum_{l=0}^{N_D}\left[\int_0^\infty ds\int_0^\infty ds_1\int_0^\infty ds_2\, e^{-\omega_s(s+s_1+s_2)}\right.\right.$$
$$\left.\left.\times\overline{V(\vec{r}-s_1\hat{k},\vec{r}+s_2\hat{k})[V(\vec{r}-s\hat{k},\vec{r})+V(\vec{r},\vec{r}+s\hat{k})]}+\text{c.c.}\right]\right\rangle. \tag{52}$$

Expanding $V$ in a Fourier series, the spatial average in Eq. (52) may be performed and $G_a^{(4)}$ takes the form

$$G_a^{(4)}=-\frac{t}{2}\sum_{l=0}^{N_D}\frac{1}{2\pi}\int_0^{2\pi}d\varphi\sum_{l,m}\int_0^\infty ds\int_0^\infty ds_1\int_0^\infty ds_2 e^{-\omega_l(s+s_1+s_2)}V_{l,m}(-(s_1+s_2)\hat{k})$$
$$\times V_{l,m}^*(s\hat{k})\cos\left(\vec{Q}_{l,m}\frac{s}{2}\hat{k}\right)\cdot\left[\cos\left(\vec{Q}_{l,m}\frac{-s_1+s_2}{2}\hat{k}\right)\cos[\mu\overline{B}(s+s_1+s_2)]\right.$$
$$\left.+\sin\left(\vec{Q}_{l,m}\frac{-s_1+s_2}{2}\hat{k}\right)\sin[\mu\overline{B}(s+s_1+s_2)]\right],$$

where $V_{l,m}$ is given by Eq. (B3) and the symmetry relations (7) have been used to rearrange the integrand. We introduce center-of-mass coordinates $t_S=s_1+s_2$, $t_R=s_1-s_2$ in the $s_1,s_2$ plane. Replacing $s_1,s_2$ by the new variables, the integration over $t_R$ may be performed and the double integral over $s$ and $t_S$ becomes a product of two independent, one-dimensional integrals. Performing this step, $G_a^{(4)}$ takes the form

$$G_a^{(4)}=-t\sum_{l=0}^{N_D}\frac{1}{2\pi}\int_0^{2\pi}d\varphi\sum_{l,m}\frac{1}{\vec{Q}_{l,m}\hat{k}}\int_0^\infty ds e^{-\omega_l s}\cos\left(\frac{s}{2}\vec{Q}_{l,m}\hat{k}\right)\cdot V_{l,m}^*(s\hat{k})\int_0^\infty dt_S e^{-\omega_l t_S}$$
$$\times\sin\left(\frac{t_S}{2}\vec{Q}_{l,m}\hat{k}\right)\cdot V_{l,m}(-t_S\hat{k})[\cos(\mu\overline{B}s)\cos(\mu\overline{B}t_S)-\sin(\mu\overline{B}s)\sin(\mu\overline{B}t_S)]. \quad (53)$$

An attempt to simplify Eq. (53) further, by performing one of the remaining integrations analytically, was not successful. At this point it seems already feasible to calculate the remaining integrals over $s,\varphi$ and the sums over Matsubara and Fourier indices numerically. However, we prefer to proceed and calculate the remaining integrals by means of an asymptotic approximation.

Let us consider for definiteness the integral over $s$ in Eq. (53). The integrand has its maximum at $s=0$. We analyze the behavior of the various factors in the integrand as a function of $s$, and neglect the $s$ dependence of the slowest varying factors. The characteristic lengths in $s$ space of the factors $\exp(-\omega_l s)$, $\cos(s\vec{Q}_{l,m}\hat{k})$, $V_{l,m}(s\hat{k})$ and $\cos(\mu\overline{B}s)$ are given by $\tau_1=[(2l+1)t]^{-1}$, $\tau_2=(\overline{B}_\perp|\vec{r}_{-l,m}|)^{-1}$, $\tau_3=(n\overline{B}_\perp)^{-1/2}$, and $\tau_4=(\mu\overline{B})^{-1}$, where $\vec{r}_{lm}=l\vec{a}+m\vec{b}$. We consider a range of inductions $\overline{B}\lesssim B_P$, where the Pauli critical field $B_P$ is (in the present system of units) given by $\mu B_P\doteq 0.4$. As a consequence, $\tau_4\gtrsim 2$. Choosing a typical number $\mu=0.1$ for the dimensionless magnetic moment, our induction varies in the range $\overline{B}\lesssim 4$. The characteristic lengths $\tau_2$ and $\tau_3$ both depend on the Landau quantum number $n$; recall that $\overline{B}_\perp$ depends on $n$ as shown in Fig. 1. Let us consider first the case $n=1$. Then, $\overline{B}_\perp\cong\overline{B}\sin\Theta_1$ with $\sin\Theta_1\approx\mu/\pi$ according to Eq. (1) and the definition of $\mu$ in Appendix A. As a consequence, $\tau_3$ is of the same magnitude as $\tau_4$ for $n=1$. The magnitude of $\tau_2\cong 7/|\vec{r}_{l,m}|$ varies strongly depending on the Fourier indices $l,m$. For not too large Fourier indices and nearly all $\omega_l$, $\tau_1$ will be the smallest of the four characteristic lengths. This is, however, only true for not too low temperatures $t$. For large Fourier indices, which should be taken into account in the present situation, the behavior of the integrand will be dominated by the term $\cos(s\vec{Q}_{l,m}\hat{k})$ because its characteristic length $\tau_2$ becomes small for large $l,m$. Thus, the latter term as well as the Matsubara term $\exp(-\omega_l s)$ has to be kept, while the terms $V_{l,m}(s\hat{k})$ and $\cos(\mu\overline{B}s)$ show the slowest variation in $s$ and may be replaced by their values at $s=0$. This conclusion remains true for arbitrary $n$. This may be seen by using the relation $n\overline{B}_\perp\cong\beta$ which will be derived in Sec. VI.

Using this asymptotic approximation both the integral over $s$ and the Fermi-surface average may be performed analytically and one arrives at the result

$$G_a^{(4)}=-\frac{t}{4}\sum_{l=0}^{N_D}\sum_{l,m}V_{l,m}^*(s\hat{k})|_{s=0}V_{l,m}(-t_S\hat{k})|_{t_s=0}$$
$$\times\frac{2\omega_l^2+\frac{1}{4}|\vec{Q}_{l,m}|^2}{\omega_l^2\left(\omega_l^2+\frac{1}{4}|\vec{Q}_{l,m}|^2\right)^{3/2}}.$$

The second nonmagnetic term $G_b^{(4)}$ [see Eq. (41)], which is evaluated with the same method, is given by $G_b^{(4)}=-2G_a^{(4)}$.

In order to calculate the fourth-order terms of magnetic origin, $G_c^{(4)}$ and $G_d^{(4)}$, the Fourier coefficients of the quantities $\eta^0$, $\vec{\beta}$ [see Eq. (50)] have to be evaluated first. This may be done using a method similar to the one outlined above for $G_a^{(4)}$. A noticeable difference is that the $s$ dependence of the slowest varying factors (the ones with characteristic lengths $\tau_3$ and $\tau_4$) cannot be completely neglected in the course of the asymptotic approximation, but must be taken into account to linear order in $s$. In a second step, Maxwell's equation has to be solved to obtain the magnetic-field correction $\vec{B}_1$. Given the latter, the free energy $G_c^{(4)}$ may be calculated. The term $G_d^{(4)}$ contains an additional $s$ integral which may be performed by means of an asymptotic approximation of the above type. The relation $G_d^{(4)}=-2G_c^{(4)}$ was again found to

be true, in analogy to the nonmagnetic case (the same relation has been found in microscopic calculations[24] of the ordinary vortex lattice near $H_{c2}$).

Collecting all fourth-order terms and attaching the factor $\epsilon^4$ one obtains the final result

$$G^{(4)}=\epsilon^4\Bigg(\frac{t}{4}\sum_{l,m} f_1^2(x_{l,m})S_{l,m}^{(1)}-\frac{t^2}{\tilde{\kappa}^2-\mu^2}{\sum_{l,m}}' [\overline{B}_\parallel^2\mu^4 f_1^2(x_{l,m}) \times (S_{l,m}^{(1)})^2+(\overline{B}_\perp\mu^2 f_1(x_{l,m})S_{l,m}^{(1)}-g_1(x_{l,m})S_{l,m}^{(2)})^2]\Bigg), \tag{54}$$

where the prime at the second summation sign indicates that the term $l=0$, $m=0$ is to be excluded from the sum. The functions $f_1$, $g_1$ depend explicitly on the Landau quantum number $n$ and are given by

$$f_1(x)=e^{-x/2}L_n(x), \tag{55}$$

$$g_1(x)=e^{-x/2}\left[\frac{1}{2}L_n(x)+(1-\delta_{n,0})L_{n-1}^1(x)\right], \tag{56}$$

where $L_n^1$ is a Laguerre polynomial.[21] The Matsubara sums are given by

$$S_{l,m}^{(1)}=\sum_{l=0}^{N_D}\frac{2\omega_l^2+\frac{1}{4}|\vec{Q}_{l,m}|^2}{\omega_l^2\left(\omega_l^2+\frac{1}{4}|\vec{Q}_{l,m}|^2\right)^{3/2}}, \tag{57}$$

$$S_{l,m}^{(2)}=\sum_{l=0}^{N_D}\frac{1}{\omega_l^2\left(\omega_l^2+\frac{1}{4}|\vec{Q}_{l,m}|^2\right)^{1/2}}. \tag{58}$$

The square of the reciprocal-lattice vector is conveniently written in the form $|\vec{Q}_{l,m}|^2=2\overline{B}_\perp x_{l,m}/2$, where $x_{l,m}$ is defined by Eq. (B4). Introducing a magnetic length $L$ defined by

$$\overline{B}_\perp=\frac{2\pi}{ab\sin\alpha}=\frac{2}{L^2}, \tag{59}$$

these parameters which depend on $a$, $b$, $\alpha$, are given by

$$x_{l,m}=\frac{\pi^2}{\sin^2\alpha}\left(\frac{L}{a}\right)^2 l^2+\left(\frac{a}{L}\right)^2 m^2-2\pi lm\frac{\cos\alpha}{\sin\alpha}. \tag{60}$$

### E. Local induction

The components $B_{1\perp}$ and $B_{1\parallel}$ of the spatially varying magnetic field $\vec{B}_1$ are given by Fourier series of the form

$$B_{1\Delta}(\vec{r})={\sum_{l,m}}' (B_{1\Delta})_{l,m}e^{\imath\vec{Q}_{l,m}\vec{r}}, \tag{61}$$

where $\Delta=\perp,\parallel$. The Fourier coefficients are given by

$$(B_{1\parallel})_{l,m}=-\frac{t\langle|\Delta_n|^2\rangle}{\tilde{\kappa}^2-\mu^2}\overline{B}_\parallel\mu^2 \times(-1)^{lm}e^{-\imath\pi l(b/a)\cos\alpha}f_1(x_{l,m})S_{l,m}^{(1)}, \tag{62}$$

$$(B_{1\perp})_{l,m}=-\frac{t\langle|\Delta_n|^2\rangle}{\tilde{\kappa}^2-\mu^2}(-1)^{lm}e^{-\imath\pi l(b/a)\cos\alpha} \times[\overline{B}_\perp\mu^2 f_1(x_{l,m})S_{l,m}^{(1)}-g_1(x_{l,m})S_{l,m}^{(2)}]. \tag{63}$$

The parallel component (62) is proportional to $\mu^2$ and is entirely due to the spin pair-breaking effect. The perpendicular component (63) is the sum of a $\mu^2$-dependent term and a second term not (explicitly) dependent on $\mu$. The terms dependent on $\mu^2$ have the same form for both components (recall that the direction of $B$ in spin space is arbitrary) and are proportional to the relevant component of the macroscopic induction. The second term in Eq. (63), which is of opposite sign, may only for $n=0$ be considered as a consequence of orbital pair breaking; for $n>0$ this second term depends also (since a positive $n$ is necessarily due to a finite $\mu$) on the spin pair-breaking effect. The GL limit of the local induction is discussed in Appendix C.

The validity of the asymptotic approximation used in the derivation of Eqs. (54) and (61) is not restricted to low $n$, but sufficiently high temperatures, say $t>0.1$, should be used. Clearly, if different states with *very small* free-energy differences are found, no conclusion as to the relative stability of these states can be drawn.

### F. Extremal conditions

In thermodynamic equilibrium, the values of $\epsilon$, $\overline{B}_\perp$, $\overline{B}_\parallel$ and the lattice parameters $a$, $b$, $\alpha$ have to be chosen in such a way that the free energy becomes minimal. To find the equilibrium values of $\epsilon$, $\overline{B}_\perp$, $\overline{B}_\parallel$ the extremal conditions

$$\frac{\partial G}{\partial\epsilon}=0,\quad \frac{\partial G}{\partial\overline{B}_\parallel}=0,\quad \frac{\partial G}{\partial\overline{B}_\perp}=0, \tag{64}$$

have to be solved near $H_{c2}$. The question for the optimal $a$, $b$, $\alpha$ will be addressed in the following section.

Inserting the superconducting solution for $\epsilon$ in the free energy yields

$$G=\overline{G}-\frac{1}{4}\frac{(\overline{G}^{(2)})^2}{\overline{G}^{(4)}}, \tag{65}$$

where the coefficients $\overline{G}$, $\overline{G}^2$, and $\overline{G}^4$ are defined by $G=\overline{G}+\epsilon^2\overline{G}^{(2)}+\epsilon^4\overline{G}^{(4)}$. Equation (65) shows, that the stable lattice structure (see Sec. IV) is determined by the requirement of minimal $\overline{G}^4$.

To find the two-component macroscopic magnetization relation between induction $\overline{B}_\perp$, $\overline{B}_\parallel$ and external field $H_\perp$, $H_\parallel$, the above extremal conditions must be solved for $\overline{B}_\perp$, $\overline{B}_\parallel$. This cannot be done for arbitrary fields but requires an appropriate expansion of the coefficients for small $\overline{B}_\perp$

$-\overline{B}_{c2,\perp}$, $\overline{B}_\parallel - \overline{B}_{c2,\parallel}$. A lengthy but straightforward calculation, generalizing Abrikosovs classical work[25] to the present situation, leads to the result

$$\overline{B}_\perp = \alpha_{\perp\perp} H_\perp + \alpha_{\perp\parallel} H_\parallel + \beta_\perp ,$$

$$\overline{B}_\parallel = \alpha_{\perp\parallel} H_\perp + \alpha_{\parallel\parallel} H_\parallel + \beta_\parallel . \tag{66}$$

The coefficients in this linear relation are given by

$$\alpha_{\perp\perp} = 2\tilde{\kappa}^2 [2(\tilde{\kappa}^2 - \mu^2) - A_\parallel]/\det M,$$

$$\alpha_{\perp\parallel} = 2\tilde{\kappa}^2 A_{\parallel\perp}/\det M,$$

$$\alpha_{\parallel\parallel} = 2\tilde{\kappa}^2 [2(\tilde{\kappa}^2 - \mu^2) - A_\perp]/\det M,$$

$$\beta_\perp = -2(\tilde{\kappa}^2 - \mu^2)(A_\perp B_{c2,\perp} + A_{\parallel\perp} B_{c2,\parallel})/\det M,$$

$$\beta_\parallel = -2(\tilde{\kappa}^2 - \mu^2)(A_\parallel B_{c2,\parallel} + A_{\parallel\perp} B_{c2,\perp})/\det M,$$

where

$$\det M = 2(\tilde{\kappa}^2 - \mu^2)[2(\tilde{\kappa}^2 - \mu^2) - A_\parallel - A_\perp].$$

The parameters $A_\parallel, \ldots$ may be calculated for a given lattice structure with the help of the relations

$$A_\parallel = \frac{1}{2\overline{G}^{(4)}} \left( \frac{\partial \overline{G}^{(2)}}{\partial \overline{B}_\parallel} \right)^2 , \tag{67}$$

$$A_\perp = \frac{1}{2\overline{G}^{(4)}} \left( \frac{\partial \overline{G}^{(2)}}{\partial \overline{B}_\perp} \right)^2 , \tag{68}$$

$$A_{\parallel\perp} = \frac{1}{2\overline{G}^{(4)}} \frac{\partial \overline{G}^{(2)}}{\partial \overline{B}_\parallel} \frac{\partial \overline{G}^{(2)}}{\partial \overline{B}_\perp} , \tag{69}$$

where the derivatives of $\overline{G}^{(2)}$ have to be evaluated at $\overline{B} = B_{c2}$ and the relation $A_\parallel A_\perp = A_{\parallel\perp}^2$ may be shown to be true.

Equation (66) constitutes the macroscopic relation between induction and external field for a 2D superconductor in a tilted magnetic field. It is, of course, strongly anisotropic and shows a coupling between the parallel and perpendicular field components. For $H_\parallel = 0$, $\mu \Rightarrow 0$, and $t \Rightarrow 1$, Eq. (66) should reduce to Abrikosov's GL solution[25,32] for the magnetization of a triangular vortex lattice. This is indeed the case as shown in Appendix C.

For $H_\parallel = 0$, $\mu \Rightarrow 0$, Eq. (66) describes the ordinary vortex lattice (near $H_{c2}$) for arbitrary temperatures. A numerical comparison with corresponding results by Eilenberger[23] and Rammer and Pesch[24] has not been undertaken because a different (spherical) Fermi surface has been used in these works. However, the limit $H_\parallel = 0$, $\mu \Rightarrow 0$ of the present theory will be checked in Appendix D by calculating the critical value of $\kappa$ separating type-II from type-I superconductivity.

## IV. RESULTS FOR FINITE PERPENDICULAR FIELD

In this section we determine the stable order-parameter structures for the paramagnetic vortex states with $1 \leqslant n \leqslant 4$ in the vicinity of $H_{c2}$. The numerical procedure to find the stable states is essentially the same as in KRS.[8] First, the upper critical field $B_{c2}$ and the corresponding quantum number $n$ have to be found for given temperature $t$ and tilt angle $\Theta$ by solving the linearized gap equation (37). In a second step, the stable lattice structure, which minimizes the fourth-order term $\overline{G}^{(4)} = G^{(4)}/\epsilon^4$ [see Eq. (54)], has to be determined. Because of the flux quantization condition the minimum with respect to only *two* parameters, which may be chosen as $a/L$ and $\alpha$, must be found. In contrast to the ordinary vortex lattice, where it is usually sufficient to calculate only a few lattices of high symmetry (triangular, quadratic) to find the stable state, the present situation is characterized by a large number of local minima of Eq. (54), corresponding to a large number of possible lattices of rather irregular shape. Therefore, a graphical method was used to determine the stable state; the free-energy surface $\overline{G}^{(4)}(a/L, \alpha)$ was plotted for the whole $(a/L, \alpha)$ plane and the global minimum was determined by inspection. Basically, two material parameters, $\mu$ and $\tilde{\kappa}$, and two externally controlled parameters, $t$ and $\Theta$, enter the theory. Numerical calculations have been performed for a single value of $\mu = 0.1$, two different reduced temperatures 0.2 and 0.5, four different values 0.1, 1.0, 10, 100 of Eilenberger's parameter $\tilde{\kappa}$, and several values of $\Theta$ corresponding to different Landau quantum numbers $n$. Some of the resulting order parameter and magnetic-field structures in the range $n \leqslant 4$ will be reported here. These low-$n$ pairing states are, of course, the most important ones from an experimental point of view.

For comparison we consider first, in Appendix D, the ordinary vortex lattice state with $n = 0$. This illustrates the method and may also be used to check the accuracy of our asymptotic approximation. The equilibrium state for low-$\kappa$ type-II superconductors is calculated and good agreement with previous theories is found for not too low temperatures.

Considering now pairing states with $n > 0$, the number of order-parameter zeros per unit cell increases clearly with increasing $n$. One finds[8] two types of minima of $\overline{G}^{(4)}(a/L, \alpha)$, isolated minima and linelike minima. The first type corresponds to ''ordinary'' 2D lattices, the second type, characterized in a contour plot [see Fig. 1 of KRS[8]] by a line of constant $a/L$ with $\overline{G}^{(4)}(a/L, \alpha)$ nearly independent of $\alpha$, corresponds to quasi-one-dimensional, or ''FFLO-like'' lattices (rows of vortices and one-dimensional FFLO-like minima alternating). A convenient way to identify the type of minimum and find its position on the $a/L$ axis is to plot the projection of the $\overline{G}^{(4)}(a/L, \alpha)$ surface on the $(\overline{G}^{(4)}, a/L)$ plane. An example for this perspective, where sections of the free-energy surface at constant $\alpha$ show up as lines, is given in Fig. 2 for $n = 7$. The $\alpha$ coordinate of a 2D minimum cannot be read off from such a plot and requires a second projection on the $(a/L, \alpha)$ plane (such as Fig. 11 or Fig. 1 of KRS[8]). The free-energy maps for other $n > 0$ states are in principle similar to Fig. 2 but the different local minima

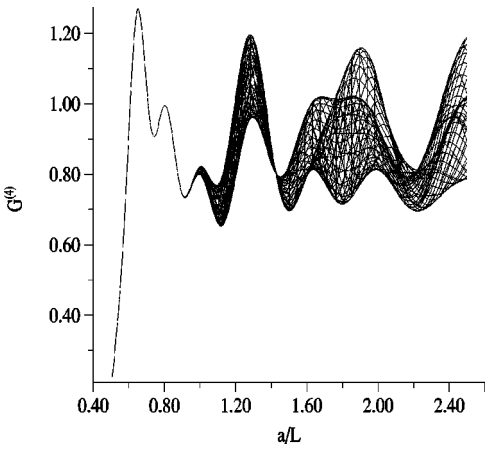


FIG. 2. Projection of the free energy $\overline{G}^{(4)}$ on the $\overline{G}^{(4)}, a/L$ plane. Using this perspective the sections of the free-energy surface at constant $\alpha$ are displayed as lines. In the considered range of $a/L$ one finds six local minima, corresponding to two FFLO-like and four two-dimensional lattices. The global minimum is at $a/L \approx 1.1$ and corresponds to a two-dimensional lattice. Parameters chosen in this plot are $n=7$, $t=0.5$, $\tilde{\kappa}=10$, $\mu=0.1$, and $\Theta=0.055$.

show more pronounced differences for smaller $n$.

Let us start with the paramagnetic vortex state with $n=1$ and consider first the limit of large $\kappa$. As reported in KRS,[8] a quasi-one-dimensional state is found to be stable in this case. Figure 3 shows the spatial variation of the modulus of the order parameter. One sees rows of vortices separated by a single, FFLO-like line of vanishing order parameter.

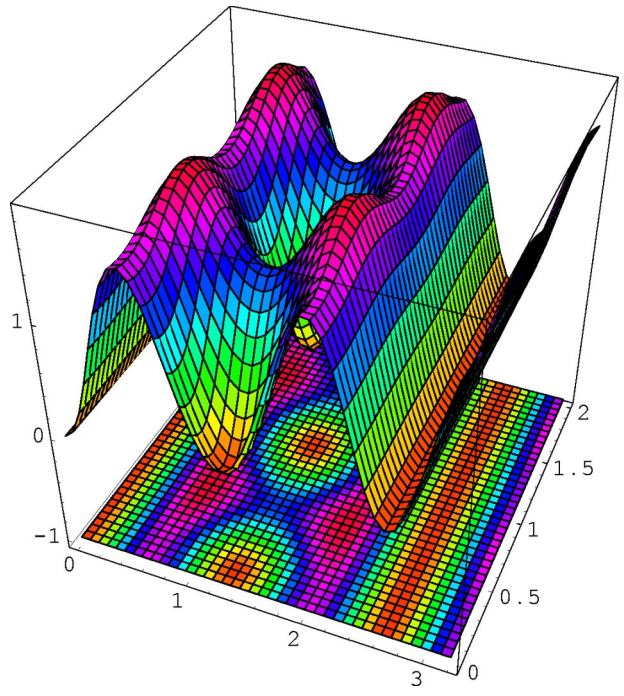


FIG. 3. (Color online) Square of modulus of order parameter $|\psi_1|^2$ as a function of $x/a$, $y/a$ in the range $0<x/a<2$, $0<y/a<3.2$. This is the stable structure (unit-cell parameters $a/b=0.205$, $\alpha=33°$) for $t=0.2$, $\tilde{\kappa}=100$, $\theta=1.2°$ ($n=1$, $B_{c2}=4.141$).

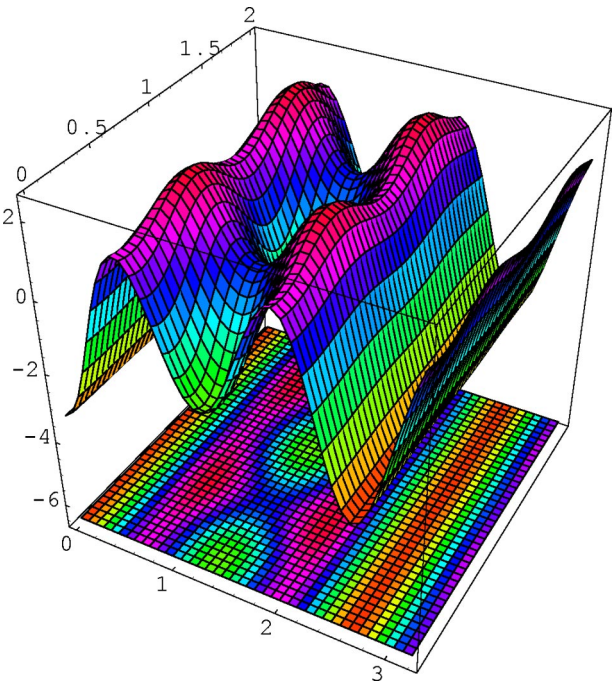


FIG. 4. (Color online) Parallel component $B_{1\|}$ as a function of $x/a$, $y/a$ in the range $0<x/a<2$, $0<y/a<3.2$. This plot has been produced using the same input parameters as in Fig. 3.

The unit cell of the structure shown in Fig. 3 is given by $a/L=1.0875$, $\alpha=33°$. A shift of the vortex rows relative to each other leads to a lattice with the same $a/L$ and a different $\alpha$, which has nearly the same free energy (which is reasonable, since the interaction between vortices from different rows is weak as a consequence of the intervening FFLO domain wall). The vortices are of the ''ordinary'' type, i.e., the phase of the order parameter changes by $+2\pi$ when surrounding the center.

It is of interest to calculate the magnetic field belonging to this order-parameter structure. We plot the parallel and perpendicular components $B_{1\|}(\vec{r})$ and $B_{1\perp}(\vec{r})$ of the spatial varying part $\vec{B}_1(\vec{r})$ of the magnetic field as given by Eqs. (61)–(63), omitting a common factor $t\langle|\Delta_n|^2\rangle/(\tilde{\kappa}^2-\mu^2)$. The field $B_{1\|}(\vec{r})$, which is entirely due to the spin pair-breaking mechanism, is shown in Fig. 4. Due to its paramagnetic nature, the field $B_{1\|}(\vec{r})$ is *expelled* from regions of small $\psi(\vec{r})$. This behavior is exactly opposite to the usual orbital response, which implies an enhancement of the induction in regions of small $|\psi|(\vec{r})$. As a consequence, the spatial variation of $B_{1\|}$ is very similar to that of $|\psi|^2$, shown in Fig. 3.

The perpendicular field $B_{1\perp}(\vec{r})$, shown in Fig. 5, consists of a spin term proportional to $\mu^2$, and a second term which does not depend [see Eq. (63)] explicitly on $\mu$. The term proportional to $\mu^2$ is negligibly small and the total field is essentially given by the second term. Near the vortices the field $B_{1\perp}(\vec{r})$ behaves in the familiar, orbital way, i.e., it is largest at the points of vanishing $\psi$ and decreases with increasing distance from the vortex centers. However, at the

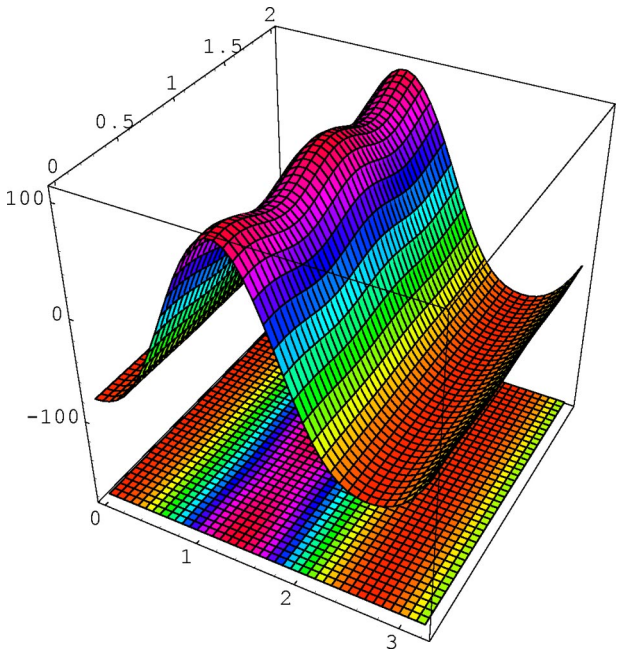


FIG. 5. (Color online) Perpendicular component $B_{1\perp}$ as a function of $x/a$, $y/a$ in the range $0<x/a<2$, $0<y/a<3.2$. The same input parameters as in Fig. 3 have been used.

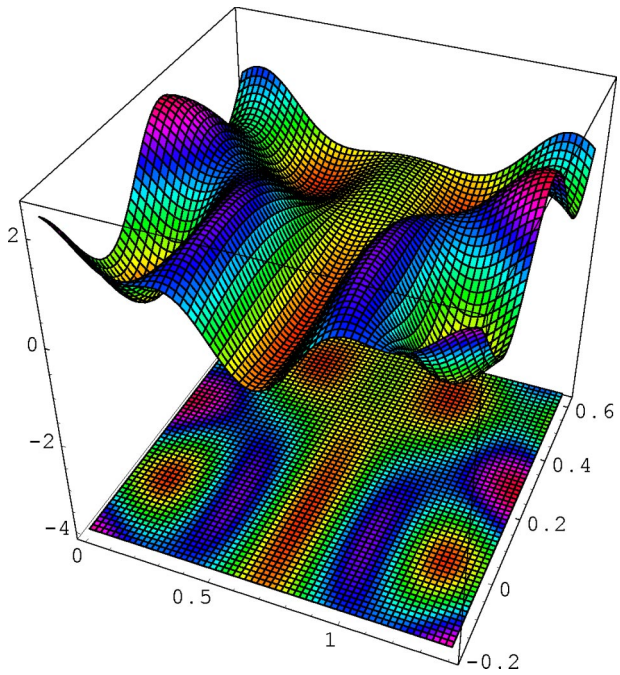


FIG. 6. (Color online) Square of modulus of order parameter $|\psi_4|^2$ as a function of $x/a$, $y/a$ in the range $0<x/a<1.4$, $-0.2<y/a<0.62$. This is the stable structure (unit-cell parameters $a/b=0.6735$, $\alpha=70.125°$) for $t=0.5$, $\tilde{\kappa}=10$, $\theta=0.1°$ ($n=4$, $B_{c2}=3.486$).

FFLO-like lines of vanishing order parameter, where no topological singularity occurs, $B_{1\perp}$ has a *minimum*, i.e., shows paramagnetic behavior. Thus, the magnetic response of a $n=1$ superconductor may either lead to a local suppression or to an enhancement of the magnetic field in regions of small order parameter. This is in contrast to the purely orbital response of a $n=0$ superconductor, where the magnetic field is always enhanced. This unconventional behavior is formally due to the second term in $g_1$ [see Eq. (56)]. The field $B_{1\parallel}$ is much smaller than $B_{1\perp}$ and the total field $B_1$ for $n=1$ is consequently dominated by the perpendicular component $B_{1\perp}$, which is a consequence of the combined action of both pair-breaking mechanisms.

The quasi-one-dimensional order-parameter structure shown in Fig. 3 seems to be representative for the pairing state with $n=1$; no other stable state has been found for $\tilde{\kappa}=10$ and $t=0.5$. At $\tilde{\kappa}=1$, 0.1 the free-energy surface has no minimum at all, which means that a transition to type-I superconductivity occurs at some value of $\tilde{\kappa}$ between 1 and 10.

Extrapolating the $n=1$ result to higher $n$, one would expect the following structure for the pairing state with Landau quantum number $n$: rows of vortices separated by $n$ lines of vanishing order parameter. Such a structure would approach the (linelike) FFLO state in the limit $n\Rightarrow\infty$. However, this simple picture is not realized, at least in the important range of low $n$. It holds generally for odd $n$, but for even $n$ *two-dimensional* structures are preferred. In the latter case, one has $n+1$ isolated order-parameter zeros per unit cell, with associated phase changes of a multiple of $2\pi$. Such a situation leads necessarily to the presence of one or more *antivortices*—vortices with a topological phase change of $-2\pi$ around the center—for states with even $n$, since the total phase change around the unit cell must remain $+2\pi$.

Recently, various proposals to create stable antivortices have been published; see, e.g., Moshkalkov and co-workers.[33] In the present context, it is clearly the strong paramagnetic pair breaking, which is responsible for the stability of the antivortices. Among the (even-$n$) antivortex states, the one with $n=2$ is most easily accessible from an experimental point of view and very stable under variations of $t$ and $\kappa$. Its properties will be discussed in detail in a separate publication;[34] a preliminary account has been published already.[35]

For $n=3$ free-energy minima for spatially varying states exist in the whole considered range $0.1\leqslant\kappa\leqslant100$ of the GL parameter. Thus, increased spin pair breaking stabilizes inhomogeneous equilibrium structures and shifts the phase boundary between type-II and type-I superconductivity to lower values of $\kappa$. In the high-$\kappa$ region (for $\kappa\geqslant10$) the stable state of a $n=3$ superconductor is of the quasi-one-dimensional type (at lower $\kappa$ a 2D state of nearly the same free energy has been found, which will not be discussed here). The fields $|\psi|^2$, $B_{1\parallel}$ look similar to the $n=1$ case (see Figs. 3 and 4) except that the vortex rows are now separated by *three* FFLO-like lines of vanishing order parameter. The vortices in neighboring rows are already completely decoupled for $n=3$; a translation of neighboring rows relative to each other changes the angle $\alpha$ between the unit-cell basis vectors but does not lead to any change (within eight digits) of the free energy. The perpendicular induction $B_{1\perp}$ is again dominated by the second term in Eq. (63) and looks similar to the $n=1$ case (see Fig. 5); in contrast to the spin part this field does not reflect the detailed order-parameter structure but has only a single broad minimum at the position of the three FFLO lines.

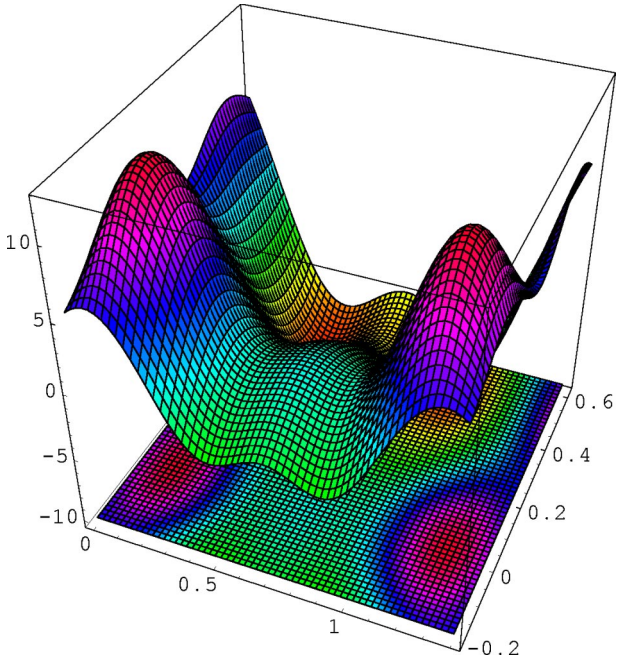


FIG. 7. (Color online) Perpendicular component $B_{1\perp}$ as a function of $x/a$, $y/a$ in the range $0<x/a<1.4$, $-0.2<y/a<0.62$. The same input parameters as in Fig. 6 have been used.

For a $n=4$ superconductor at $t=0.5$ the equilibrium state is of the quasi-one-dimensional type for $\kappa \leqslant 1$, and of the 2D type for $\kappa \geqslant 10$. Figure 6 shows the 2D order-parameter structure for a superconductor with $\kappa=10$. There are five zeros of $\psi$ per unit cell, one of them of an elongated shape. The nature of these topologically singular points may be clarified by plotting either the phase[35] or the local magnetic field. The parallel component $B_{1\parallel}(\vec{r})$ of the field $\vec{B}_1(\vec{r})$ is again (compare Figs. 3 and 4) similar in shape to the order parameter $|\psi|^2$ and need not be displayed here. The perpendicular field $B_{1\perp}$ is shown in Fig. 7. Three of the five order-parameter zeros displayed in Fig. 6 belong to "ordinary" vortices, with local-field enhancement and diamagnetic screening current (two of the three maxima of $B_{1\perp}$ are pronounced, while the third, the one corresponding to the elongated zero of $\psi$, is rather flat). The remaining two order-parameter zeros belong to antivortices with opposite sign of the "screening currents" (which are now paramagnetic in nature) and with minima of $B_{1\perp}$ at the points of vanishing $\psi$.

Results for $n>4$ will not be reported here. Many interesting and complex structures may be produced for larger $n$. However, the number of different states with similar free energies increases with increasing $n$. As a consequence, the approximate nature of our analytical calculation does not allow an identification of the stable state for large $n$. At the same time, an experimental verification of these large-$n$ states seems difficult since a very precise definition of the tilt angle $\theta$ would be required.

## V. STRUCTURE OF THE FFLO STATE

The stable state in the purely paramagnetic limit $n\to\infty$ has been determined first by Larkin and Ovchinnikov[2] at $T=0$ for a spherical Fermi surface. They predicted a one-dimensional periodic order-parameter structure of the form $\Delta(\vec{r})\approx\cos(\vec{q}\vec{r})$, which will be referred to as LO state. Later, various analytical investigations of the stable states in the vicinity of $T_{tri}$ and near $T=0$ have been performed;[36,37] many other references may be found in a recent review article.[38] A careful search for the state of lowest free energy, comparing several possible lattices in the whole temperature range, has been reported by Shimahara.[39] He found that below $t=0.24$ various 2D periodic states have lower free energy than the one-dimensional $\cos(\vec{q}\vec{r})$ state. Shimahara uses the same cylindrical Fermi surface as we do and his results do therefore apply to the present problem. Nevertheless, we reconsider in this section the problem of the determination of the FFLO structure, in order to have a complete description of all states in a tilted field in a single theoretical (quasiclassical) framework.

The results derived in Sec. III cannot be used to perform the limit $n\to\infty$ and determine the stable state in the purely paramagnetic limit. However, the general formalism may be applied in a straightforward way to the simpler case of vanishing vector potential. In order to be able to compare with previously published results we neglect in this section the possibility of spatial variations of $\vec{B}$ and restrict ourselves to the high-$\kappa$ limit.

The space of basis functions, which has to be used to expand all variables near $H_{FFLO}(T)$, is now given by the infinite set $\exp(\imath\vec{q}\vec{r})$ with a fixed value of $|\vec{q}|$. Usually, one assumes that the order parameter $\Delta$ fulfills some further symmetry (or simplicity) requirements, which then leads to a strong decrease of the number of unknown coefficients. Following this convention, we restrict ourselves to two- and one-dimensional periodic structures. For $\Theta>0$, the order parameter is not periodic but changes its phase by certain factors under translations between equivalent lattice points. These phase factors are proportional to the perpendicular induction [cf. Eq. (35)] and vanish for $\Theta\to 0$. Thus, the assumption of a periodic order parameter for $\Theta=0$ is reasonable (though not stringent). It implies, that all allowed wave vectors in the expansion of $\Delta$ must be vectors of a reciprocal lattice.

A further slight simplification stems from the behavior of the quasiclassical equations under the transformation $\vec{r}\Rightarrow -\vec{r}$, $\vec{k}\Rightarrow -\vec{k}$, which implies that the order parameter must be either even or odd under a space inversion $\vec{r}\Rightarrow -\vec{r}$. Thus, the order parameter may be written as an infinite sum,

$$\Delta(\vec{r})=\sum_m \Delta_m e^{\imath\vec{Q}_m\vec{r}}, \tag{70}$$

with coefficients defined by

$$\Delta_m=|\Delta|\sum_{i=1}^{I} c_i(\delta_{m,n_i}\pm\delta_{m,-n_i}). \tag{71}$$

Here, a shorthand notation $m$ is used for the two integers characterizing a 2D reciprocal-lattice vector $\vec{Q}_m$ [cf. the Fourier expansion at the beginning of Appendix B]. The vectors

actually entering the expansion are distinguished by an index $i$, their total number is $I$, and the two integers characterizing $\vec{Q}_{n_i}$ are denoted by $n_i$. The complex numbers $c_i$ are the expansion coefficients; one may set $c_1=1$ since only the relative weight is important. It turns out that the two solutions distinguished in Eq. (71) by a sign are essentially equivalent, and only one of them, say the even one, need be considered. Thus, the order parameter becomes a linear combination of cosine functions.

All reciprocal-lattice vectors used in Eq. (70) must be of the same length. Denoting this length by $q(T)$, the condition $|\vec{Q}_m|=q(T)$ takes the form

$$\left(\frac{l}{\tilde{a}}\right)^2\frac{1}{\sin^2\alpha_p}+\left(\frac{j}{\tilde{b}}\right)^2\frac{1}{\sin^2\alpha_p}-2\frac{lj}{\tilde{a}\tilde{b}}\frac{\cos\alpha_p}{\sin^2\alpha_p}=1, \quad (72)$$

where the two integers $l$, $j$ have been used here to represent the double index $m$. The dimensionless quantities $\tilde{a}$, $\tilde{b}$ are defined by $\tilde{a}=q(T)a_p/2\pi$, $\tilde{b}=q(T)b_p/2\pi$, where $a_p$, $b_p$, $\alpha_p$ denote the lattice parameters in the paramagnetic limit. If $I$ reciprocal-lattice vectors exist, the lattice parameters $a_p$, $b_p$, $\alpha_p$, fulfill $I$ relations like Eq. (72) with $I$ pairs of integers $l_1,j_1,\ldots,l_I,j_I$.

Using Eq. (70) the free-energy expansion near $H_{FFLO}(T)$, including terms of fourth order in the small amplitude $|\Delta|$, may be performed by means of methods similar to Sec. III. The result for the purely paramagnetic free energy $G_p$ takes the form

$$G_p=\overline{G}_p+G_p^{(2)}+G_p^{(4)}, \quad (73)$$

where $\overline{G}_p=-\mu^2H^2$, and $G_p^{(2)}$ and $G_p^{(4)}$ are contributions of order $|\Delta|^2$ and $|\Delta|^4$, respectively.

The second-order term is given by

$$G_p^{(2)}=|\Delta|^2\sum_{i=1}^{I}|c_i|^2\overline{A}, \quad (74)$$

with the $i$-independent coefficient $\overline{A}$ defined by

$$\overline{A}=2\left(\ln t+t\int_0^\infty ds\frac{1-e^{-\omega_D s}}{\sinh st}[1-\cos(\mu\overline{B}s)J_0(sq)]\right).$$

The condition $\overline{A}=0$ determines the upper critical field; it may also be derived from Eq. (37), performing the limit $n\to\infty$.

The fourth-order term is given by

$$G_p^{(4)}=|\Delta|^4\left[\sum_{i=1}^{I}|c_i|^4\overline{A}_i+\sum_{i\neq k}^{I}|c_i|^2|c_k|^2\overline{B}_{i,k}+\sum_{i\neq k}^{I}[(c_i^*)^2(c_k)^2+\text{c.c.}]\overline{C}_{i,k}\right], \quad (75)$$

$G_p^{(4)}$ depends on the lattice structure via the coefficients $\overline{A}_i$, $\overline{B}_{i,k}$, and $\overline{C}_{i,k}$, which are defined by

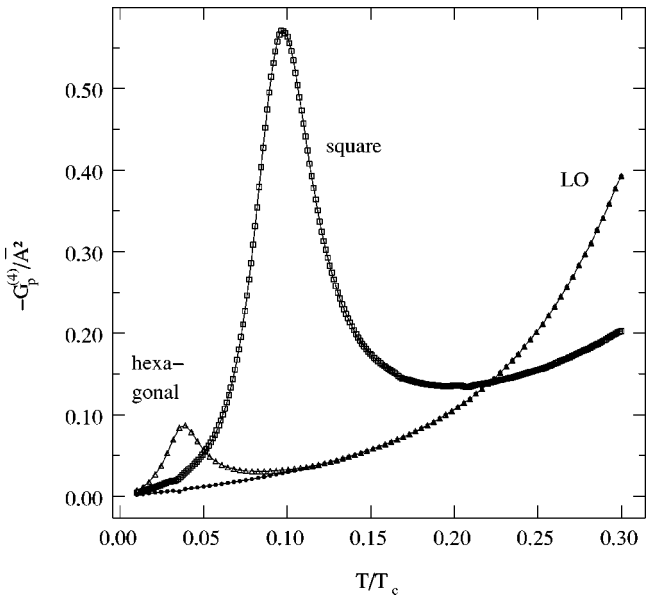


FIG. 8. The fourth-order term $G_p^{(4)}$ (minimized with respect to $|\Delta|$) divided by $-\overline{A}^2$ [see Eq. (74)] at $H_{FFLO}(T)$ for three different periodic structures as a function of reduced temperature $t=T/T_c$. The part of the hexagonal curve which is lower than the LO state is not visible, since the coefficients $c_i$ are determined automatically to yield the highest possible solution for $-G_p^{(4)}/\overline{A}^2$.

$$\overline{A}_i=\frac{t}{2}\sum_{l=0}^{N_D}\int_0^{2\pi}\frac{d\varphi}{2\pi}[P_{n_i,n_i,n_i}(\hat{k})+2P_{n_i,-n_i,-n_i}(\hat{k})],$$

$$\overline{B}_{i,k}=\frac{t}{2}\sum_{l=0}^{N_D}\int_0^{2\pi}\frac{d\varphi}{2\pi}2[P_{n_i,n_k,n_k}(\hat{k})+P_{n_i,-n_k,-n_k}(\hat{k})],$$

$$\overline{C}_{i,k}=\frac{t}{2}\sum_{l=0}^{N_D}\int_0^{2\pi}\frac{d\varphi}{2\pi}P_{-n_k,-n_i,n_k}(\hat{k}),$$

where

$$P_{n_1,n_2,n_3}(\hat{k})=\frac{1}{N_{n_1}^-N_{n_2}^-N_{n_3}^-}+\frac{1}{N_{n_1}^+N_{n_2}^+N_{n_3}^+},$$

$$N_n^\pm=\omega_l+\imath[\pm\mu\overline{B}+\vec{Q}_n\hat{k}].$$

In contrast to Eq. (54) no approximations have been used in deriving Eq. (75).

Using Eq. (72) all possible 2D lattices and wave vectors may be calculated numerically. The stable lattice at $H_{FFLO}(T)$ is then determined from the condition of lowest $G_p^{(4)}$, taking also the LO state into consideration. It turns out that it is energetically favorable at $H_{FFLO}(T)$ if all eigenfunctions in the order parameter expansion (70) have equal weight, i.e., $c_i=1$ for all $i$.

The result of the numerical search for the lowest free energy of periodic structures, characterized by maximal three pairs of reciprocal wave vectors, is displayed in Fig. 8. The highest curve at a given temperature corresponds to the stable lattice. For $0.22<t<0.56$ the one-dimensional LO

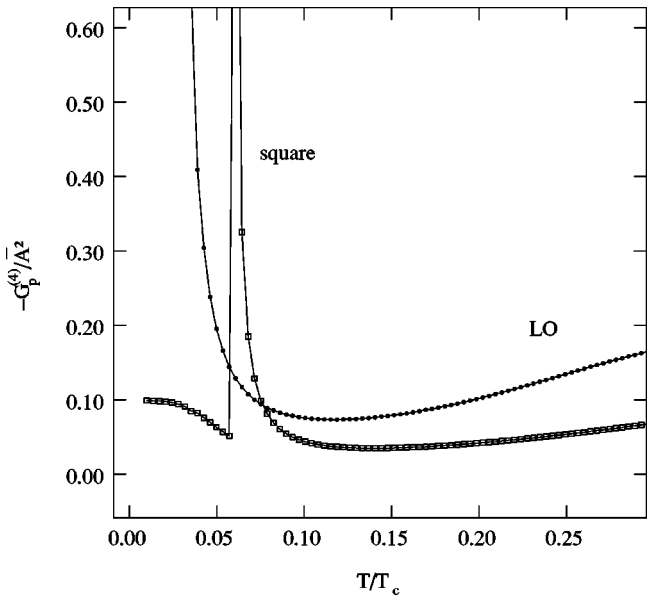


FIG. 9. The term $-G_p^{(4)}/\overline{A^2}$ for the LO state and the square state at $0.90H_{FFLO}(T)$, as a function of reduced temperature $T/T_c$. The hexagonal curve is lower than the LO state and is not displayed in this figure.

state is realized. For $t<0.22$ 2D periodic structures appear, namely the square state for $0.05<t<0.22$, and the hexagonal state for $t<0.05$ (we use here the notation of Shimahara[39] for the 2D states). Besides the fact that the triangular state[39] is absent, because it is neither even nor odd, the present results agree quantitatively with those of Shimahara,[39] obtained within a different, but equivalent, formalism. Thus, more complicated 2D periodic structures than those found already in Ref. 39 do not exist in the considered range of temperatures; the assumption of equal weight for different wave vectors [$c_i=1$ for all $i$ in Eq. (71)] has also been confirmed for these states.

The temperature region *below* $t=0.01$ has been investigated recently by Mora and Combescot.[37] They found a series of states characterized by an even (total) number $2N=8,10,\ldots$ of different wave vectors, all entering the order-parameter expansion with equal weight, and with $N$ increasing with decreasing temperature. Merging these results with the present ones, one obtains a very simple description of all of the FFLO states at the phase boundary, namely an infinite number of states, each one being a linear combination of $N=1,2,\ldots$ cosine functions of equal weight and with $N$ different, but equally spaced, wave vectors.

Of course, it is also of interest to investigate the possible equilibrium structures in the region *below* the critical field. As a first step in this direction, preliminary calculations at $0.95H_{FFLO}$ and $0.90H_{FFLO}$ have been performed, using the fourth-order expansion (73), which is not valid near first-order transition lines. The result is surprising and shows a revival of the LO state in the low-temperature region.

In Fig. 9 the terms $-G_p^{(4)}/\overline{A^2}$, for the three states displayed in Fig. 8, are plotted as a function of temperature *below* the transition line, at $0.9H_{FFLO}$. The hexagonal state (not visible) does not exist any more. The usual square state (characterized by $c_i=1$) is only stable in a very small temperature interval $0.061<t<0.075$. The LO state is now stable in a much larger interval $0.075<t<0.56$, as compared to Fig. 8. It is also stable in a small temperature region below $t=0.061$. But at $t\approx 0.017$ the factor $-G_p^{(4)}/\overline{A^2}$ for the LO state has a singularity and jumps from $+\infty$ to $-\infty$. This implies that the fourth-order term (for the LO state) changes sign and that a first-order transition occurs somewhere in the vicinity of this singularity; higher-order terms in the free energy would be required for a quantitative treatment. Between this singularity at $t\approx 0.017$ and the lowest considered temperature $t=0.01$ the stable state is again characterized by a square unit cell. However, the order parameter in this temperature range, $0.01<t<0.017$, is given by a linear combination of plane-wave states [see Eqs. (70) and (71)] with a real coefficient $c_1=1$ and an *imaginary* coefficient $c_2=\imath$. The usual order-parameter structure for the square lattice, which is characterized by two real weight factors of equal magnitude ($c_1=c_2=1$), is not equivalent to this case and has higher free energy.

The results below $H_{FFLO}(T)$ indicate that the 2D states are only stable in a tiny interval near the phase boundary, and that the one-dimensional LO state reappears inside the superconducting state. The square state—the one with the smallest $N$ ($N=2$)—has the largest stability region, as one would also expect from the free-energy balance shown in Fig. 8. We shall come back to the question of the stability of the 2D states in Sec. VI, considering it from a different point of view. In this context it seems worth mentioning that terms up to eighth order with respect to the order parameter must be taken into account, in order to describe the FFLO phase transition of a *three-dimensional* superconductor in the framework of GL theory.[40] The structure found below the singular point of the LO state (see Fig. 9) raises the question, whether still other order-parameter structures, different from those found at the transition line, will appear near $t=0$ deep in the superconducting state. The present fourth-order expansion is not really appropriate to answer this question.

## VI. TRANSITION TO THE PURELY PARAMAGNETIC REGIME

The limit $n\to\infty$ of the series of paramagnetic vortex states, discussed in Sec. IV, is now well known; for $0.22<t<0.56$ the one-dimensional LO state is realized, while 2D states of square or hexagonal type, predicted by Shimahara,[39] appear at lower $t$. The region of still smaller $t$, below $t=0.01$, which has been studied by Mora and Combescot,[37] will not be considered here. The way this limit is approached, is, however, unknown. Thus, we address ourselves in this section to the question of *how* the one- or two-dimensional unit cell of the FFLO state develops from the unit cell of the paramagnetic vortex states if the Landau-level index $n$ tends to infinity.

This limiting process is very interesting, because a vast number of different states with different symmetry is passed through in a small interval of tilt angles $\theta$. The unit cell of the *finite-n* states is subject to the condition that it carries exactly a single quantum of flux of the perpendicular field

$B_\perp$. Since $B_\perp \to 0$ as $n \to \infty$, at least one of the unit-cell vectors must approach infinite length—i.e., the dimension of the macroscopic sample—in this limit. Thus, the $n \to \infty$ limiting process describes a transition from a microscopic (or mesoscopic) length scale to a macroscopic length scale.

The transition to the FFLO state has previously been investigated by Shimahara and Rainer[4] in the linear regime. They found the important relation

$$q = \lim_{n\to\infty} \sqrt{4eB_\perp n/\hbar c}, \tag{76}$$

where $q$ is the absolute value of the FFLO wave vector (here we changed to ordinary units). Equation (76) has been derived by identifying the asymptotic form of the Hermite polynomials[21] with the form of the LO order parameter. It implies that a relation

$$B_\perp \approx \frac{\beta}{n}, \quad \beta = \frac{\hbar c q^2}{4e} \tag{77}$$

holds at large $n$. The validity of Eq. (76) may also be checked numerically by comparing the numbers $\beta$ and $q$, which are both obtained from the upper critical-field equation.

Relation (77) may be derived from basic physical properties of the present system. The energy spectrum for planar Cooper pairs in a perpendicular magnetic field $B_\perp$ is the same as for electrons and is given by

$$E_n = \hbar\omega\left(n + \frac{1}{2}\right), \quad \omega = \frac{eB_\perp}{mc}. \tag{78}$$

Considering now the energy spectrum of Cooper pairs for $B_\perp = 0$, one has to distinguish two cases. First, in the common situation without a large spin pair-breaking field, all Cooper pairs occupy the lowest possible energy $E=0$, which is the kinetic energy $p^2/4m$ taken at the Cooper pair momentum $p=0$. Second, if a large spin pair-breaking field parallel to the conducting plane exists, the energy value to be occupied by the Cooper pairs, shifts to a finite value $p^2/4m$, since the Cooper pairs acquire a finite momentum $p$ due to the Fermi-level shift discussed in Sec. I. Thus, in the latter case, which is of interest here, the Landau levels (78) must obey the condition

$$E_n = \frac{\hbar e}{mc} B_\perp \left(n + \frac{1}{2}\right) \underset{B_\perp \to 0}{\to} \frac{p^2}{4m} \tag{79}$$

for $B_\perp \to 0$. If $p$ is replaced by the wave number $q = p/\hbar$, Eq. (77) becomes equivalent to Eq. (79). The limiting behavior expressed by Eq. (76) or Eq. (77) is therefore a direct consequence of Landau's result for the energy eigenvalues of a charged particle in a magnetic field.

Combining Eq. (77) with analytical results at $T=0$, the limiting behavior of the unit cell as $n \to \infty$ may be understood. Expressing the FFLO wave number in terms of the BCS coherence length $\xi_0$ by means of the relation $q = (2/\pi)\xi_0^{-1}$, and using the flux quantization condition in the form

$$F^{(n)} B_\perp^{(n)} = \Phi_0 \tag{80}$$

[with $\Phi_0 = hc/2e$ and $B_\perp$ defined by Eq. (77)] the area $F^{(n)}$ of the unit cell for pairing in Landau level $n$ is approximately given by

$$F^{(n)} \doteq \pi^3 \xi_0^2 n. \tag{81}$$

Thus, the unit-cell area diverges with the first power of $n$. The behavior of the magnetic length $L$, which is defined by the relation $B_\perp = (\Phi_0/\pi)L^{-2}$, is given by $L \doteq \pi\xi_0 n^{1/2}$.

Equation (81) is not sufficient to determine the shape of the unit cell in the limit of large $n$. However, a simple possibility to produce a one-dimensional periodic LO structure for $n \to \infty$ is a divergence of one of the unit-cell lengths, say $b$, of the form $b \approx n$, while the second length $a$ remains constant, i.e., $a \approx n^0$. The numerical results for the states referred to in Sec. IV as "FFLO-like," or quasi-one-dimensional states show a behavior

$$\frac{a}{L} \doteq \frac{\chi}{\sqrt{n}}, \tag{82}$$

which is in agreement with this possibility. The numerical value of the constant $\chi$ is close to $2\sqrt{2}$, which corresponds to $a = 2\pi\xi_0$ and to the lattice constant $\pi/q$ of the LO state. Thus, the LO state may be identified as the limiting case of the quasi-one-dimensional states of Sec. IV for large $n$; the distance of the FFLO lines is essentially independent of $n$, while the periodicity length $b \sin\alpha$ in the direction perpendicular to the lines tends to infinity (like $b \sin\alpha \doteq n\pi/q$) for $n \to \infty$. The one-dimensional FFLO unit cell is a *substructure* that develops inside the diverging unit cell of the paramagnetic vortex states.

To complete the description of the transition to the LO state, the above lattice structure may be used in Eq. (16) to perform the limit $n \to \infty$ of the order-parameter expansion $\Delta_n$. We consider a 2D sample of *finite* area $F_p$, which contains $N_a N_b$ "small" unit cells of size $F_c = ab \sin\alpha$. The total area is given by $F_p = L_a L_b \sin\alpha$ with $L_a = N_a a$ and $L_b = N_b b$. For different $n$ the size and shape of $F_c$ may change while $F_p$ remains, of course, unchanged. Adopting the above model for the behavior of the unit cell as a function of $n$, we have $n$-independent numbers $N_a$ and $a$, while $b = b^{(n)}$ increases linearly with $n$ and $N_b = N_b^{(n)}$ decreases consequently according to

$$N_b^{(n)} = \frac{L_b}{b^{(n)}} = \frac{2L_b \sin\alpha}{\pi^2 \xi_0} \frac{1}{n}. \tag{83}$$

Thus, a largest possible Landau number $n = n_c$ exists, which corresponds to $b^{(n_c)} = L_b$ (or $N_b^{(n_c)} = 1$) and is given by

$$n_c = \frac{2L_b \sin\alpha}{\pi^2 \xi_0}. \tag{84}$$

This cutoff $n_c$ agrees exactly, in the present model, with the number of $n=1$ unit cells fitting into a length $L_b$. As an additional consequence of the finite area of the sample, only

a finite number of terms occur in the sum over $m$ in Eq. (16). This number is fixed by the condition that the ''center positions'' $y_m = mb \sin\alpha = m\pi L^2/a$ lie inside the sample.[22] This leads to the condition

$$-\frac{aL_b \sin\alpha}{2L^2\pi} \leqslant m < \frac{aL_b \sin\alpha}{2L^2\pi}, \tag{85}$$

which is in the limit $n = n_c$ only fulfilled for $m = 0$. Using the asymptotic expansion[21] of the Laguerre polynomial $L_n$, for large and even $n = 2j$, and taking into account only the term with $m = 0$ in the sum of Eq. (16), the order parameter takes the form

$$\Delta_{2j} \approx AC_{2j}D_j \cos\left(\frac{\sqrt{8j}}{L}y\right). \tag{86}$$

The amplitude $A$ [see Eq. (15)] is, in the present system of (ordinary) units, given by

$$A = \left(\frac{2B_\perp}{\Phi_0 L_a^2}\right)^{1/4}.$$

The coefficient $C_{2j}$ is, in the limit $n \to n_c$, simply given by $C_{2j} = (F_p)^{1/2}$ [see Eq. (17)], and the coefficient $D_j$ takes the form

$$D_j = \frac{2^j (j-1)!}{(-1)^j \sqrt{2\pi(2j-1)!}}.$$

While these factors, $A$, $D_j$, $C_{2j}$ diverge for $n \to \infty$, if the sample dimensions approach infinity, all singularities cancel if $n$ is replaced by the cutoff $n_c$, and one obtains the expected result, $\Delta_{n_c} = \cos qy$, for the one-dimensional periodic order-parameter structure in the purely paramagnetic limit.

The transition to the *two-dimensional* (square and hexagonal) periodic states found by Shimahara[39] is more involved than the transition to the LO state. Let us restrict to the square state, which is the simplest of all 2D states, and is also most stable from a thermodynamic point of view.

For the square state, which is a linear combination of two LO states with orthogonal wave vectors, one would expect a divergent behavior of *both* unit-cell basis vectors of the type $a \approx n^{1/2}$, $a = b \approx n^{1/2}$. Consequently, choosing a square unit cell in the (exact) order-parameter expansion, Eq. (18), one would expect to find a substructure which becomes increasingly similar, with increasing $n$, to the structure of Shimahara's square state (linelike order-parameter zeros, in the form of two sets of orthogonal straight lines and circles). Numerical calculations, performed in the range $n < 40$ are, however, not in agreement with this expectation.

On the other hand, the mathematical limit of the order parameter (18) yields, in fact, a 2D state with the periodicity of the FFLO wave vector and square symmetry, as shown in Appendix E for a simplified model. The explanation for this apparent contradiction is provided by the result [relation (E8) of Appendix E] that the quantum number $n$ for a square state must obey the condition $n = \pi N^2$, where $N$ is an integer. This is a general result, which has been derived using essentially only the behavior $a \approx n^{1/2}$ for large $n$. The latter is a consequence of the flux quantization condition and the shape of the unit cell.

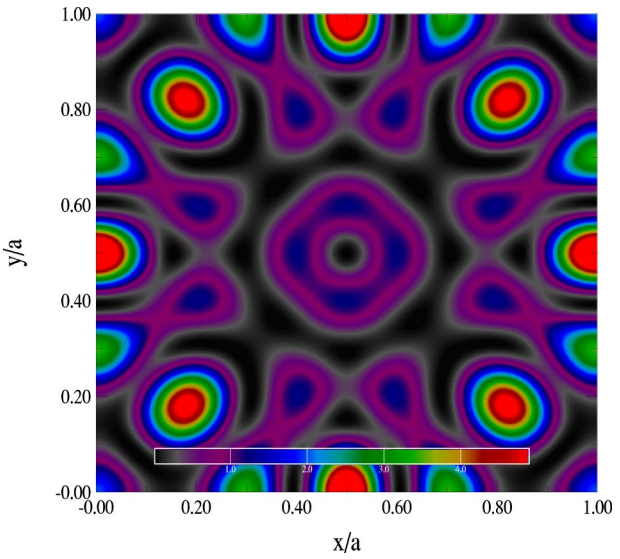


FIG. 10. (Color online) Contour plot of the square of the order-parameter modulus for Landau quantum number $n = 28$ and a unit cell with parameters $a = b$, $\alpha = \pi/2$.

Of course, the relation $n = \pi N^2$ cannot be fulfilled exactly for finite numbers $n$, $N$ (for a sample of finite extension) since $\pi$ is an irrational number. The proper meaning of this relation is that the sequence of states with quantum numbers $n = int(\pi N^2)$, $N = 1,2,\ldots$ represents a sequence of approximations (of increased quality) to the square state. Thus, the square state is the limit of a sequence defined on a very *small* subset of the set of integer numbers.

This explains why no systematic development of the square state with increasing $n$ has been observed in the numerical calculations. The largest quantum number in the considered range ($n < 40$), which fulfills the above condition is $n = 28$ (corresponding to $N = 3$). The order-parameter modulus for $n = 28$ is shown in Fig. 10. It reveals, in fact, a certain similarity to the structure of the square state (at least more similarity than any other state in the considered range). The arrangement of isolated order parameter zeros in Fig. 10 shows a tendency towards the formation of linelike zeros. Clearly, an extremely high $n$ and an extremely sharp definition of the tilt angle would be required to produce a really good approximation to the square state. The final conclusion of the present analysis for the square state, that extreme requirements with regard to the definition of the tilt angle must be fulfilled in order to produce it, will probably hold for all other 2D states as well.

The above analysis of the formation of the FFLO state(s) as limit(s) of the paramagnetic vortex states for $n \to \infty$ has been based on relation (79). In addition, relation (79) allows for an intuitive understanding of the unusual phenomenon of Cooper pairing at higher $n$, encountered in the present configuration. The choice $n = 0$ for the ordinary vortex state—in the absence of paramagnetic pair breaking—corresponds to the lowest energy the system can achieve for $p = 0$. For suf-

ficient large $H_\parallel$ and decreasing $H_\perp$, the Landau-level spacing becomes smaller than the kinetic energy and the system has to perform a quantum jump from the $n=0$ to the $n=1$ pairing state, in order to fulfill the requirement of given energy as close as possible within the available range of discrete states [inserting $n=1$ in Eq. (79) determines the angle $\theta_1$ as given by Eq. (1)]. For the same reason, a series of successive transitions to superconducting states of increasing $n$ takes place with further decreasing $H_\perp$, until the FFLO state is finally reached at $B_\perp=0$. The FFLO state for $n\to\infty$ may obviously be considered as the continuum limit, or quasiclassical limit, of this series of Cooper-pair states, which starts with the ordinary vortex state at $n=0$.

## VII. CONCLUSION

The paramagnetic vortex states studied here, appear in a small interval of tilt angles close to the parallel orientation. A common feature of all of these states is a finite momentum of the superconducting pair wave function, which is due to the large parallel component of the applied magnetic field. In these new superconducting states the Cooper pairs occupy quantized Landau levels with nonzero quantum numbers $n$. The number $n$ increases with decreasing tilt angle and tends to infinity for the parallel orientation, where the FFLO state is realized. The unusual occupation of higher Landau levels may be understood in terms of the finite momentum of the Cooper pairs.

The end points of the infinite series of Cooper-pair wave states occupying different $n$ are the ordinary vortex state at $n=0$ and the FFLO state at $n=\infty$. The dominant pair-breaking mechanism in the vortex state is the orbital effect, while Cooper pairs can only by broken by means of the spin effect in the FFLO state. The equilibrium structure of the new states, which occupy the levels $0<n<\infty$, is very different from the structure of the FFLO state(s), despite the fact that the difference in tilt angles and phase boundaries may be small. Generally speaking, the equilibrium structures of the new states reflect the presence of *both* pair-breaking mechanisms; the fact that the local magnetic response may be diamagnetic or paramagnetic depending on the position in the unit cell may be understood in terms of this competition. A second unusual property, also closely related to the simultaneous presence of both pair-breaking mechanisms, is the coexistence of vortices and antivortices in a single unit cell.

The FFLO state has been predicted in 1964 and a large number of experimental and theoretical works dealing with this effect have been published since then. A definite experimental verification has not been achieved by now. However, recent experiments in the organic superconductor $\kappa$-$(BEDT\text{-}TTF)_2Cu(NCS)_2$ and other layered materials[41–44] revealed remarkable agreement[46,45,47] with theory, both with regard to the angular and the temperature dependence of the upper critical field. In these phase boundary experiments, identification of the FFLO precursor states, studied in the present paper, seems possible if the tilt angle is defined with high precision. Very recently, by means of heat capacity and magnetization measurements, two transition lines have been found in the heavy-fermion superconductor $CeCoIn_5$ which may be interpreted as upper and lower critical fields of the FFLO state.[48] On top of that, varying the direction of the applied field, a series of phase transitions has been observed,[48] which might be related to the paramagnetic vortex states studied in the present paper. Of course, the heavy-fermion material $CeCoIn_5$ differs considerably from the simple superconducting material, with isotropic gap and cylindrical Fermi surface, studied here. However, some general features of the present theory, such as coexisting vortices and antivortices or coexisting linelike and pointlike order-parameter zeros, can be expected to remain valid. To obtain the most direct evidence for all of these unconventional states, including the FFLO limit, other experiments, such as measurements of the local density of states by means of a scanning tunneling microscope would be useful.

## ACKNOWLEDGMENTS

I would like to thank D. Rainer, Bayreuth, and H. Shimahara, and Hiroshima for useful discussions and helpful comments during the initial phase of this work.

## APPENDIX A: SYSTEM OF UNITS AND NOTATION

In this appendix we use primes to distinguish Eilenberger's dimensionless quantities, which will be used in Secs. III–V, from ordinary ones. The primes will be omitted in Secs. III–V.

Temperature: $t=T/T_c$.

Length: $\vec{r}\,'=\vec{r}/R_0$, $R_0=\hbar v_F/2\pi k_B T_c=0.882\xi_0$, $\xi_0$ is the BCS coherence length.

Fermi velocity: $\hat{v}_F=\vec{v}_F/v_F$.

Wave number: $k'=kR_0$.

Matsubara frequencies: $\omega_l'=\omega_l/\pi k_B T_c=(2l+1)t$.

Order parameter: $\Delta'=\Delta/\pi k_B T_c$.

Magnetic field: $\vec{H}'=\vec{H}/H_0$, where $H_0=\hbar c/2eR_0^2$.

Vector potential: $\vec{A}'=\vec{A}/A_0$, where $A_0=\hbar c/2eR_0$.

Magnetic moment: $\mu'=\mu/\mu_0=\pi k_B T_c/mv_F^2$, where $\mu_0=\pi k_B T_c/H_0$. Note that the dimensionless magnetic moment $\mu'$ *agrees with the quasiclassical parameter*.

Gibbs free energy: $G'=G/[(\pi k_B T_c)^2 N_F R_0^3]$.

Eilenberger's parameter $\tilde{\kappa}$ is related to the GL parameter $\kappa_0$ of a clean superconductor according to the relation $\tilde{\kappa}=[7/18\zeta(3))]^{1/2}\kappa_0=0.6837\kappa_0$.

The symbol $\hat{k}$ denotes a dimensionless, 2D unit vector. The Fermi-surface average of a $\hat{k}$-dependent quantity $a(\hat{k})$ is denoted by $\overline{a}$. For our cylindrical Fermi surface this average is simply an integral from 0 to $2\pi$ over the azimuth angle $\varphi$.

$$\overline{a}=\frac{1}{4\pi}\oint d^2\hat{k}\,a(\hat{k})=\frac{1}{2\pi}\int_0^{2\pi}d\varphi a[\hat{k}(\varphi)].$$

Finally, the symbol $\langle a\rangle$, defined by

$$\langle a\rangle=\frac{1}{F_c}\int_{unit\ cell}d^2r\,a(\vec{r}),$$

denotes a spatial average of a quantity $a(\vec{r})$ over a unit cell of area $F_c$.

### APPENDIX B: GAP CORRELATION FUNCTION

It is convenient to express the gap correlation function, defined by Eq. (35) in terms of center-of-mass coordinates $\vec{R}=(\vec{r}_1+\vec{r}_2)/2$, $\vec{r}=\vec{r}_1-\vec{r}_2$, using the notation $V^{CM}(\vec{R},\vec{r})=V(\vec{r}_1,\vec{r}_2)$. The function $V^{CM}(\vec{R},\vec{r})$ is invariant under center-of-mass translations $\vec{R}\Rightarrow\vec{R}+l\vec{a}+j\vec{b}$ and may consequently be expanded in a Fourier series, using reciprocal-lattice vectors $\vec{Q}_{l,j}=l\vec{Q}_1+j\vec{Q}_2$, $l,j=0,\pm1,\pm2,\ldots$, with basis vectors

$$\vec{Q}_1=\frac{2\pi}{a}\begin{pmatrix}1\\ -\frac{1}{\tan\alpha}\end{pmatrix},\vec{Q}_2=\frac{2\pi}{b}\begin{pmatrix}0\\ \frac{1}{\sin\alpha}\end{pmatrix}.$$

The Fourier coefficients of $V^{CM}(\vec{R},\vec{r})$ are denoted by $V_{l,j}(\vec{r})$. The Fourier transform of $V_{l,j}(\vec{r})$ with respect to $\vec{r}$ is denoted by $V_{l,j}^{(p)}(\vec{p})$.

Using the behavior of the gap $\Delta(\vec{r})$ under lattice translations $\vec{r}\Rightarrow\vec{r}+\vec{r}_{l,j}$, where $\vec{r}_{l,j}=l\vec{a}+j\vec{b}$, the important relation

$$V_{-l,j}(\vec{r})=e^{\imath\pi l[j+(b/a)\cos\alpha]}V_{0,0}(\vec{r}+\vec{r}_{j,l}) \tag{B1}$$

may be proven. This relation, first reported by Delrieu,[49] shows that all Fourier coefficients are known if $V_{0,0}$ is known. A similar relation holds for the Fourier transform $V_{l,j}^{(p)}$:

$$V_{l,j}^{(p)}(\vec{p})=e^{\imath\vec{p}\vec{r}_{j,-l}-\imath\pi l[j+(b/a)\cos\alpha]}V_{0,0}^{(p)}(\vec{p}).$$

The functions $V_{l,j}$ and $V_{l,j}^{(p)}$, which are most useful for the evaluation of the free energy, may be calculated by proceeding along the chain

$$V^{CM}(\vec{R},\vec{r})\Rightarrow V_{0,0}(\vec{r})\Rightarrow V_{0,0}^{(p)}(\vec{p})\Rightarrow V_{l,j}^{(p)}(\vec{p})\Rightarrow V_{l,j}(\vec{r}),$$

where an arrow denotes either calculation of a Fourier coefficient or of a Fourier transform, or application of Delrieu's relation.

Using the order-parameter expansion (16) and performing the necessary manipulations, the result for $V_{l,j}^{(p)}$ is given by

$$V_{l,j}^{(p)}(\vec{p})=\frac{4\pi}{\overline{B}_\perp}(-1)^{n+lj}\langle|\Delta_n|^2\rangle e^{-\vec{p}^2/\overline{B}_\perp}L_n\left(\frac{2}{\overline{B}_\perp}\vec{p}^2\right)\times e^{-\imath\pi n(b/a)\cos\alpha}e^{\imath(F_C/2\pi)(p_xQ_{l,j,y}-p_yQ_{l,j,x})}, \tag{B2}$$

where $Q_{l,j,x}$, $Q_{l,j,y}$ are the $x$ and $y$ components, respectively, of the reciprocal-lattice vector $\vec{Q}_{l,j}$. The final result for $V_{l,j}$ is given by

$$V_{l,j}(\vec{r})=(-1)^{lj}\langle|\Delta_n|^2\rangle e^{-\imath\pi n(b/a)\cos\alpha}e^{-(\overline{B}_\perp/4)G_{l,j}^2}\times L_n\left(\frac{\overline{B}_\perp}{2}G_{l,j}^2\right), \tag{B3}$$

$$\frac{\overline{B}_\perp}{2}G_{l,j}^2=\frac{\pi}{F_C}\vec{r}^2+xQ_{l,j,y}-yQ_{l,j,x}+x_{l,j},$$

$$x_{l,j}=\frac{\pi}{\sin\alpha}\left[\left(\frac{b}{a}\right)l^2+\left(\frac{a}{b}\right)j^2-2lj\cos\alpha\right]. \tag{B4}$$

The usefulness of the gap correlation function for pair-wave states with arbitrary $n$ is essentially based on the translational invariance of the observable quantities $|\psi|$ and $B$.

### APPENDIX C: THE GINZBURG-LANDAU LIMIT

Let us first consider the upper critical field $H_{c2}^{GL}$, which is determined by $\overline{G}^{(2)}=0$, for $\mu=0$, $n=0$ ($H_\parallel=0$), and $t\rightarrow1$. Solving this equation in this limit, one finds, using ordinary units,

$$H_{c2}^{GL}=1.222\frac{\Phi_0}{2\pi\xi_0^2}(1-t). \tag{C1}$$

Equation (C1) differs from the usual GL result by a factor of 3/2. This discrepancy is due to our use of a cylindrical Fermi surface, instead of a spherical one, and can be eliminated by replacing the GL parameter $\kappa$ by $3\kappa_{GL}/2$ (the quantities used in Eilenberger units are derived assuming a spherical Fermi surface).

The magnetization relation (66) takes the following form for $H_\parallel=0$, $\mu=0$, $t\rightarrow1$:

$$\overline{B}-H=4\pi M=\frac{H-H_{c2}}{2\tilde{\kappa}^2/A_\perp-1}. \tag{C2}$$

The coefficient $A_\perp$ in Eq. (C2) is given by Eq. (68). The fourth-order free-energy contribution (54) takes the form

$$\overline{G}^{(4)}=\frac{S^{(1)}}{4}\left[\sum_{l,m}f_1^2(x_{l,m})-\frac{S^{(1)}}{4\tilde{\kappa}^2}\sum_{l,m}{}'f_1^2(x_{l,m})\right], \tag{C3}$$

where $S^{(1)}=7\zeta(3)/8$. The first sum in Eq. (C3) turns out to agree with Abrikosov's geometrical factor $\beta_A$,

$$\sum_{l,m}f_1^2(x_{l,m})=\beta_A, \tag{C4}$$

as discussed in more detail in KRS.[8] Performing again the above replacement of $\kappa$ one arrives at Abrikosov's well-known result

$$4\pi\left.\frac{\partial M}{\partial H}\right|_{H_{c2}}=\frac{1}{(2\kappa_{GL}^2-1)\beta_A}. \tag{C5}$$

Equation (C4) remains also valid for $n>0$. For the nonmagnetic terms in Eq. (54), the Matsubara sum $S_{l,m}^{(1)}$ may be

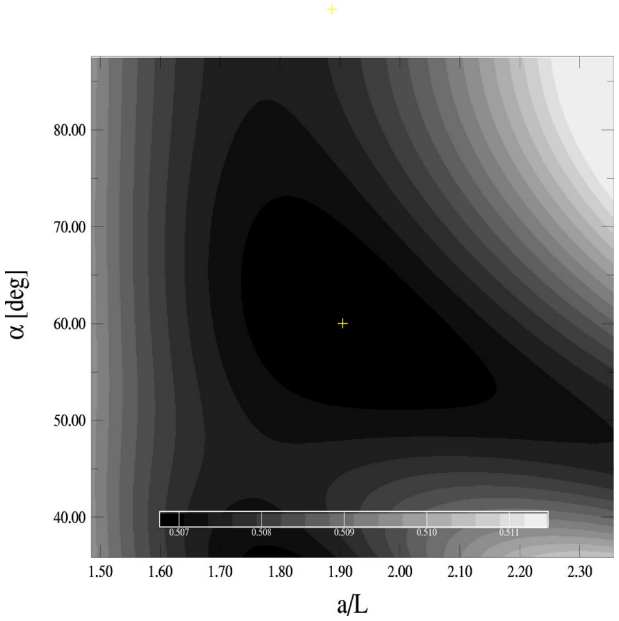


FIG. 11. Contour plot of the free energy $G^{(4)}$ as a function of $a/L$ and $\alpha$ without paramagnetic pair breaking. Parameters are $\tilde{\kappa}=1.5$, $t=0.5$, $\mu=0$, and $\Theta=\pi/2$. The minimal value $G^{(4)}=0.5067$ is at $a/L=1.905$, $\alpha=60$.

considered as a low-temperature correction to the GL term (C4). The GL limit of the local magnetic field $B_{1\perp}$ [see Eq. (63)] has also been calculated and has been found to obey the correct GL relation[32] between magnetic field and square of order parameter. Here, the low-temperature corrections are contained in the Matsubara sum $S^{(2)}_{l,m}$.

## APPENDIX D: THE LIMIT OF THE ORDINARY VORTEX LATTICE

It is of interest to investigate the limit of Eq. (54) corresponding to the ordinary vortex lattice. We consider a situation without paramagnetic pair breaking, i.e., set $\mu=0$, $\Theta=\pi/2$, and ask for the equilibrium structure of the vortex lattice and the critical value of $\kappa$ separating type-I from type-II superconductivity. To compare with the usual notation, we use here the same scaling $\kappa\Rightarrow 2\kappa/3$ of the GL parameter as in Appendix C. Figure 11 shows the free energy $G^{(4)}$ as a function of $a/L$, $\alpha$ for $\kappa=1.46$ ($\tilde{\kappa}=1.5$) at $t=0.5$. The flat minimum of $G^{(4)}$ at $a/L=1.905$, $\alpha=60$ indicates that the stable configuration is, as expected, a triangular vortex lattice. No other local minimum of the free energy exists. With decreasing $\kappa$ this minimum changes quickly into a maximum; below $\kappa\doteq 1.36$ the free energy has no minimum at all, which means that no spatially varying superconducting state exists. The critical value of $\kappa\doteq 1.36$ separating type-I from type-II behavior at $t=0.5$ agrees fairly well with the result of $\kappa\doteq 1.25$ obtained by Kramer[50] for the phase boundary between type-II and type-II/I behavior. For lower temperature the agreement is worse; at $t=0.2$ the present theory gives $\kappa=2.5$ while Kramer's theory[50] gives $\kappa=1.7$. Recall that the error induced by the asymptotic approximation of Sec. III D increases with decreasing temperature.

## APPENDIX E: THE SQUARE LIMIT FOR A MODEL ORDER PARAMETER

The square of the order parameter modulus, Eq. (18), for a square lattice may be written in the form

$$|\psi_n|^2(x,y,a)=\sum_{l,j} H_{l,j},$$

$$H_{l,j}=(-1)^{lj}e^{-(\pi/2)(l^2+j^2)}L_n(\pi(l^2+j^2))e^{\imath(2\pi/a)(lx+jy)}. \tag{E1}$$

We are interested in the limiting behavior of Eq. (E1) for $n\to\infty$, $a\approx n^{1/2}\to\infty$. In this limit, the quantity $2\pi/a$ tends to zero and the double sum may be approximated by a double integral. An appropriate tool to perform such a calculation for infinite sums in a systematic way is Poisson's summation formula. Using a two-dimensional version, which is derived in exactly the same way as for single sums, Eq. (E1) may be written in the form

$$|\psi_n|^2(x,y,a)=\left(\frac{a}{2\pi}\right)^2\sum_{m_x}\sum_{m_y}\int dk'_x\int dk'_y e^{-\imath(m_xk'_x+m_yk'_y)} \times h(k'_x,x,k'_y,y,a), \tag{E2}$$

where $h(k_x,x,k_y,y,a)$ is a function representing $H_{l,j}$. The problem here is the factor $(-1)^{lj}$ [see Eq. (E1)], which must be represented by an infinite series of step functions.[51]

Since we are more interested in the question *if* a limit with the correct periodicity and symmetry exists, than in the detailed functional form of this limit, we represent the factor $(-1)^{lj}$ approximately by the real part of $\exp\imath a^2k_xk_y/4\pi$, i.e., we use the function

$$h(k_x,x,k_y,y,a)=H_{l,j}|_{l=(a/2\pi)k_x,j=(a/2\pi)k_y} \tag{E3}$$

to represent $H_{l,j}$. Using this model, the absolute value of the rhs of Eq. (E2) will be denoted by $S(x,y,a)$ instead of $|\psi_n|^2(x,y,a)$. It takes the form

$$S(x,y,a)=\left(\frac{a}{2\pi}\right)^2\left|\sum_{m_x}\sum_{m_y}\int dk'_x\int dk'_y \times h(k'_x,x-m_xa,k'_y,y-m_ya,a)\right|, \tag{E4}$$

where $h(k_x,x,k_y,y,a)$ is given by

$$h(k_x,x,k_y,y,a)=\cos\left(\frac{a^2}{4\pi}k_xk_y\right)e^{-(a^2/8\pi)(k_y^2+k_y^2)} \times L_n\left(\frac{a^2}{4\pi}(k_y^2+k_y^2)\right)e^{\imath(k_xx+k_yy)}.$$

In order to perform the integrations, the relation

$$L_n(x+y)=\frac{1}{(-1)^n 2^{2n} n!}\sum_{m=0}^{n}\binom{n}{m}H_{2m}(\sqrt{x})H_{2n-2m}(\sqrt{y}).$$

may be used to rewrite the Laguerre polynomial in the integrand as a sum of products depending on $k_x$ and $k_y$ separately. Then, the integration over $k_x$ may be performed[21] and, after a simple shift of the integration variable, a second relation[52]

$$(-2)^n H_n\left(\frac{x+y}{\sqrt{2}}\right)H_n\left(\frac{x-y}{\sqrt{2}}\right)=\sum_{m=0}^{n}(-1)^m\binom{n}{m}H_{2m}(\sqrt{x})H_{2n-2m}(\sqrt{y})$$

may be used to calculate the sum over $m$. Performing the integration over $k_x$ one obtains the final result

$$S(x,y,a)=\left|\frac{\imath^n}{\sqrt{2}2^n n!}\sum_{m_x}\sum_{m_y}e^{-(\pi/a^2)\tilde{x}^2}H_n\left(\frac{\sqrt{2\pi}}{a}\tilde{x}\right)\times e^{-(\pi/a^2)\tilde{y}^2}H_n\left(\frac{\sqrt{2\pi}}{a}\tilde{y}\right)(e^{-\imath(2\pi/a^2)\tilde{x}\tilde{y}}+(-1)^n e^{\imath(2\pi/a^2)\tilde{x}\tilde{y}})\right|, \quad \text{(E5)}$$

where the abbreviations $\tilde{x}=x-m_x a$, $\tilde{y}=y-m_y a$ have been used.

We are interested in the limiting value of Eq. (E5) for $n\to\infty$. The asymptotic behavior of the Hermite polynomials[21] for large $n$ implies

$$H_n\left(\frac{\sqrt{2\pi}}{a}\tilde{x}\right)\approx\cos\left[(2n+1)^{1/2}\frac{\sqrt{2\pi}}{a}x-(2n+1)^{1/2}\sqrt{2\pi}m_x\right]. \quad \text{(E6)}$$

Since $a\approx n^{1/2}$, the factor in front of $x$ in Eq. (E6) remains finite for $n\to\infty$ and defines the FFLO wave vector $q$, i.e.,

$$(2n+1)^{1/2}\frac{\sqrt{2\pi}}{a}=q \quad \text{for} \quad n\to\infty. \quad \text{(E7)}$$

Equation (E7) implies a restriction on the possible quantum numbers $n$ of a square FFLO state. The fact that an integer number $N$ of wavelengths $\lambda=2\pi/q$ must fit into a length $a$ implies the condition

$$n=\pi N^2 \quad \text{(E8)}$$

in the limit $a\to\infty$. Condition (E8) is of a general nature and not a specific feature of our model. For quantum numbers $n$ obeying Eq. (E8), all $(m_x,m_y)$-dependent phase factors in Eq. (E6) become multiples of $2\pi$ and may be omitted. The limit of $S(x,y,a)$ for $a\to\infty$ obtained in this way is well defined, i.e., independent of any cutoff, and is given by

$$\lim_{n\to\infty}S(x,y,a)\approx|\cos(qx)\cos(qy)|. \quad \text{(E9)}$$

A rotation of $\pi/4$ transforms Eq. (E9) into the more familiar form[39] $|\cos(q'x')+\cos(q'y')|$. The expected correct result for $|\psi_n|^2$ is the *square* of the rhs of Eq. (E9). Thus, the result of our model calculation differs from the exact result. A limiting state of the correct periodicity and symmetry has, however, been obtained.

*Email address: ulf.klein@jku.at


[1] P. Fulde and R.A. Ferrell, Phys. Rev. **135**, A550 (1964).
[2] A.I. Larkin and Y.N. Ovchinnikov, Sov. Phys. JETP **20**, 762 (1965).
[3] L.N. Bulaevskii, Sov. Phys. JETP **38**, 634 (1974).
[4] H. Shimahara and D. Rainer, J. Phys. Soc. Jpn. **66**, 3591 (1997).
[5] B.S. Chandrasekhar, Appl. Phys. Lett. **1**, 7 (1962).
[6] A.M. Clogston, Phys. Rev. Lett. **9**, 266 (1962).
[7] H. Burkhardt and D. Rainer, Ann. Phys. **3**, 181 (1994).
[8] U. Klein, D. Rainer, and H. Shimahara, J. Low Temp. Phys. **118**, 91 (2000).
[9] M. Rasolt and Z. Tesanovic, Rev. Mod. Phys. **64**, 709 (1992).
[10] J.C. Ryan and A.K. Rajagopal, Phys. Rev. B **47**, 8843 (1993).
[11] H. Akera, A.H. MacDonald, S.M. Girvin, and M.R. Norman, Phys. Rev. Lett. **67**, 2375 (1991).
[12] Z. Tesanovic, M. Rasolt, and L. Xing, Phys. Rev. Lett. **63**, 2425 (1989).
[13] C.T. Rieck, K. Scharnberg, and R.A. Klemm, Physica C **170**, 195 (1990).
[14] V.N. Nicopoulos and P. Kumar, Phys. Rev. B **44**, 12080 (1991).
[15] S. Manalo and U. Klein, Phys. Rev. B **65**, 144510 (2002).
[16] K. Gloos, R. Modler, H. Schimanski, C.D. Bredl, C. Geibel, F. Steglich, A.I. Buzdin, N. Sato, and T. Komatsubara, Phys. Rev. Lett. **70**, 501 (1993).
[17] G. Eilenberger, Z. Phys. **214**, 195 (1968).
[18] A.I. Larkin and Y.N. Ovchinnikov, Sov. Phys. JETP **28**, 1200 (1969).
[19] J.A.X. Alexander, T.P. Orlando, D. Rainer, and P.M. Tedrow, Phys. Rev. B **31**, 5811 (1985).
[20] G. Sarma, J. Phys. Chem. Solids **24**, 1029 (1963).
[21] I. S. Gradshteyn and I. M. Ryshik, *Table of Integrals Series and Products* (Academic Press, New York, 1965).
[22] R. E. Prange and S. M. Girvin, *The Quantum Hall Effect* (Springer, New York, 1990).
[23] G. Eilenberger, Phys. Rev. **153**, 584 (1967).
[24] J. Rammer and W. Pesch, J. Low Temp. Phys. **77**, 235 (1989).
[25] A.A. Abrikosov, Sov. Phys. JETP **5**, 1174 (1957).
[26] C.T. Rieck, K. Scharnberg, and N. Schopohl, J. Low Temp. Phys. **84**, 381 (1991).
[27] U. Klein (unpublished).
[28] G. Eilenberger, Z. Phys. **180**, 32 (1964).
[29] U. Klein, J. Low Temp. Phys. **69**, 1 (1987).
[30] U. Klein, Phys. Rev. B **40**, 6601 (1989).
[31] E. Helfand and N.R. Werthamer, Phys. Rev. **147**, 288 (1966).
[32] D. Saint-James, G. Sarma, and E. J. Thomas, *Type II Superconductivity* (Pergamon Press, Oxford, 1969).
[33] V.R. Misko, V.M. Fomin, J.T. Devreese, and V.V. Moshchalkov, Phys. Rev. Lett. **90**, 147003 (2003).
[34] U. Klein (unpublished).
[35] U. Klein, Physica C **388-389**, 651 (2003).
[36] A.I. Buzdin and M.L. Kulic, J. Low Temp. Phys. **54**, 203 (1984).
[37] C. Mora and R. Combescot, cond-mat/0306575 (unpublished).
[38] R. Casalbuoni and G. Nardulli Rev. Mod. Phys. **76**, 263 (2004).

[39] H. Shimahara, J. Phys. Soc. Jpn. **67**, 736 (1998).
[40] S. Matsuo, S. Higashitani, Y. Nagato, and K. Nagai, J. Phys. Soc. Jpn. **67**, 280 (1997).
[41] M.S. Nam, J.A. Symington, J. Singleton, S.J. Blundell, A. Ardavan, J.A.A.J. Perenboom, M. Kurmoo, and P. Day, J. Phys.: Condens. Matter **11**, L477 (1999).
[42] J. Singleton, J.A. Symington, M.S. Nam, A. Ardavan, M. Kurmoo, and P. Day, J. Phys.: Condens. Matter **12**, L641 (2000).
[43] F. Zuo, J.S. Brooks, R.H. McKenzie, J.A. Schlueter, and J.M. Williams, Phys. Rev. B **61**, 750 (2000).
[44] Y. Shimojo, T. Ishiguro, H. Yamochi, and G. Saito, J. Phys.: Condens. Matter **71**, 1716 (2002).
[45] S. Manalo and U. Klein, J. Phys.: Condens. Matter **12**, L471 (2000).
[46] H. Shimahara, J. Phys. Soc. Jpn. **71**, 1644 (2002).
[47] H. Shimahara, Physica B **329-333**, 1442 (2003).
[48] H.A. Radovan, N.A. Fortune, T.P. Murphy, S.T. Hannahs, E.C. Palm, S.W. Tozer, and D. Hall, Nature (London) **425**, 51 (2003).
[49] J.M. Delrieu, J. Low Temp. Phys. **6**, 197 (1972).
[50] L. Kramer, Z. Phys. **258**, 367 (1973).
[51] P. L. Walker, in *Mathematical Analysis and its Applications (Kuwait, 1985)*, KFAS Proceedings Series Vol. 3 (Pergamon, New York, 1988), pp. 199–210.
[52] H. Buchholtz, *The Confluent Hypergeometric Function* (Springer, Berlin, 1969).